Page intentionally left blank.

Chapter 3—Outline

Aberrations—Third Order

Page intentionally left blank.

Chapter 3
Aberrations—Third Order

3.1 Introduction

Ideally, all rays that leave an object point and pass through an optical system should pass through the same image point. Unfortunately, only when the rays are paraxial do they very nearly pass through the same image point; this image point we shall call the paraxial image point, and the plane that contains this point and is normal (or perpendicular) to the symmetry axis (the z axis) we shall call the paraxial image plane. The paraxial image point and the paraxial image plane are convenient references by which to judge aberrations. As the rays deviate from their paraxial nature, they begin to miss the paraxial image point more and more. Paraxial rays travel close to the symmetry axis in the meridional plane (the yz plane), which means that they have a small direction angle C; for the other direction angles, $A = \pi/2$ rad and $B = \pi/2 - C$. As the rays become nonparaxial, or skew, the direction angle C moves away from a value close to zero, and the direction angles A and B can also deviate from their paraxial values. In this chapter we want to study the properties of such rays.

Frequently, when we have a situation like the one we have just described, where a quantity (C in this case) starts near zero and then gets larger, a power series (or series expansion) can provide a great deal of insight into the behavior of the physics. Some series expansions that are often used are listed below with x as the small quantity.

binomial power series:

$$(1+x)^n = 1 + nx + \frac{n(n-1)}{2!}x^2 + \mathrm{O}(x^3) \qquad (3.1)$$

sine power series:

$$\sin x = x - \frac{x^3}{3!} + \frac{x^5}{5!} + \mathrm{O}(x^7) \qquad (3.2)$$

cosine power series:

$$\cos x = 1 - \frac{x^2}{2!} + \frac{x^4}{4!} + \mathrm{O}(x^6) \qquad (3.3)$$

In the above expressions, a term like $\mathrm{O}(x^3)$ stands for the rest of the infinite number of terms in the series, the first term of which has x^3 in it; it is convenient to read "$\mathrm{O}(x^3)$" as "order of x^3." The terms $\mathrm{O}(x^7)$ and $\mathrm{O}(x^6)$ are given similar explanations. It is important to realize that x in the above expansions represents a number smaller than one, so that the succeeding terms involving x^2, x^3, and higher powers, get smaller and smaller.

In our study of aberrations in this chapter, our basic expressions are power series written to the third order; thus, this study of aberrations is called third-order theory. The higher order terms are therefore of the form $\mathrm{O}(x^4)$, or if there is no fourth order, then $\mathrm{O}(x^5)$. There are five aberration classes in third-order theory:

1) spherical aberration
2) coma
3) astigmatism
4) curvature of field
5) distortion

3.2 Derivation of the Power-Series Equations

3.2.1 Translation to the refracting surface

A large amount of algebraic manipulation is involved in developing third-order theory; therefore, it helps to simplify our working diagram as much as possible. As shown in Figure 3.1, we work with a single refracting surface of radius r. This refracting surface is centered on the z axis at the vertex V. The object is a point P on the negative y axis a distance h below the origin; thus, $h < 0$ so that the paraxial image point P' (not shown in the diagram) is a positive distance h' above the z axis for a real image. Because the final equations we derive will have terms with h' in them, not h, they will be easier to analyze when $h' > 0$. As shown in the diagram, the ray starts at the point P and traverses a distance T to the point P_1 on the refracting surface of radius r. The point P_1 is also on a circle, whose radius we shall call R; this circle is an imaginary one on the refracting surface. We should regard the ray shown as one of a cone of rays that emanate from P and travel to different points on the circle of radius R. Both R and h play the role of small terms which start out near zero and then get larger so that we can see the effect they have on image aberrations.

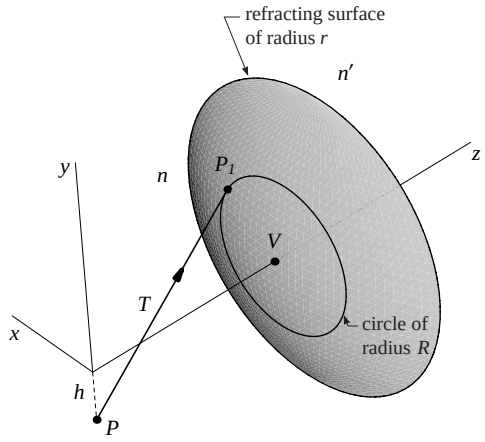

Figure 3.1

So that we can more clearly see the meaning of the terms we shall use, we redraw our previous diagram as a line drawing in Figure 3.2. The ray begins at the object point P which has an object distance ℓ, where $\ell < 0$ because P is to the left of the vertex V. Since $t > 0$, we must write $t = -\ell$, as shown in the diagram. To control where the point P_1 is on the circle of radius R, we use the angle ϕ; or in other words, we give the location of the point P_1 in polar coordinates.

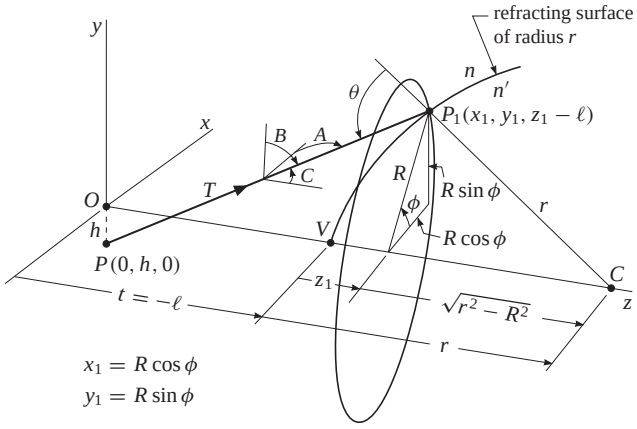

Figure 3.2

Instead of explicitly using the direction angle C, or its direction cosine γ, it is much more convenient to express γ (as well as α and β) in terms of the small quantities R and h. However, these quantities may have values greater than one, which makes it impossible to use them in a power series. To ensure that we have quantities that are smaller than one, we divide them by quantities that are larger, such as r and ℓ; thus R/r, R/ℓ, h/r, and h/ℓ are examples of quantities smaller than one that will play the role of x in Equations 3.1, 3.2, and 3.3. We shall represent any of these small quantities by simply writing s. It is much more advantageous to make the expansions in terms of these small quantities rather than the direction angle C, which is the small quantity that we originally mentioned in the Introduction.

Because we are interested in third-order theory, we explicitly write out what the small terms s equal or represent to powers of three; beyond powers of three we simply write the terms as $\mathrm{O}(s^4)$ or higher.

To begin we write an expression for z_1 by inspection of Figure 3.2, and then develop it into a series by using the binomial power series Equation 3.1:

$$z_1 = r - \sqrt{r^2 - R^2} = r\left\{1 - \left[1 - \left(\frac{R}{r}\right)^2\right]^{\frac{1}{2}}\right\}$$

$$= r\left\{1 - \left[1 - \frac{1}{2}\left(\frac{R}{r}\right)^2 + \mathrm{O}(s^4)\right]\right\}$$

$$= \frac{R^2}{2r} + r\,\mathrm{O}(s^4) \tag{3.4}$$

where in this equation s stands for the small quantity R/r. Next we use Figure 3.2 and Pythagorean's theorem to get an expression for T:

$$T = \sqrt{x_1^2 + (y_1 - h)^2 + (z_1 - \ell)^2}$$

$$= \sqrt{(R\cos\phi)^2 + (R\sin\phi - h)^2 + (z_1 - \ell)^2}$$

$$= \sqrt{R^2 - 2\sin\phi\, Rh + h^2 + \ell^2 - 2\ell z_1 + z_1^2}$$

$$= \sqrt{\ell^2\left(1 + \frac{R^2}{\ell^2} - 2\sin\phi\frac{Rh}{\ell^2} + \frac{h^2}{\ell^2} - \frac{2z_1}{\ell} + \frac{z_1^2}{\ell^2}\right)}$$

$$= -\ell\sqrt{1 + \frac{R^2}{\ell^2} - 2\sin\phi\frac{Rh}{\ell^2} + \frac{h^2}{\ell^2} - \frac{2z_1}{\ell} + \frac{z_1^2}{\ell^2}} \tag{3.5}$$

where we have used the trig identity $\sin^2\phi + \cos^2\phi = 1$. Also, it is important to note that $\sqrt{\ell^2} = -\ell$ because $\ell < 0$.

Next we substitute Equation 3.4 into the two terms involving z_1 in Equation 3.5 to get

$$-\frac{2z_1}{\ell} + \frac{z_1^2}{\ell^2} = -\frac{2}{\ell}\left[\frac{R^2}{2r} + r\,\mathrm{O}(s^4)\right] + \frac{1}{\ell^2}\left[\frac{R^2}{2r} + r\,\mathrm{O}(s^4)\right]^2$$

$$= -\frac{R^2}{\ell r} + \frac{R^4}{4\ell^2 r^2} + \frac{R^2}{\ell^2}\mathrm{O}(s^4) - \frac{2r}{\ell}\mathrm{O}(s^4) + \frac{r^2}{\ell^2}\mathrm{O}(s^8)$$

$$= -\frac{R^2}{\ell r} + \mathrm{O}(s^4) \tag{3.6}$$

To understand how we obtained Equation 3.6 in its final form, we look at each of the terms in detail. For the first term, we have

$$-\frac{R^2}{\ell r} = -\left(\frac{R}{\ell}\right)\left(\frac{R}{r}\right) = -(s)(s) = \mathrm{O}(s^2)$$

We note that the minus sign is absorbed into the order term. Because this term is of order s^2, we keep the term in its R form in Equation 3.6. For the next two terms, we have

$$\frac{R^4}{4\ell^2 r^2} = \frac{1}{4}\left(\frac{R^2}{\ell^2}\right)\left(\frac{R^2}{r^2}\right) = \frac{1}{4}(s^2)(s^2) = \mathrm{O}(s^4)$$

$$\frac{R^2}{\ell^2}\mathrm{O}(s^4) = s^2\mathrm{O}(s^4) = \mathrm{O}(s^6)$$

where the $1/4$ is absorbed into the order term; thus, it is acceptable to place constants, as well as minus signs, into an order term. Since both these terms are of order higher than s^3, they are not written out, but simply left in the order form.

The last two terms are somewhat different because terms of O(1) (read order one) arise:

$$-\frac{2r}{\ell}\mathrm{O}(s^4) = \mathrm{O}(1)\mathrm{O}(s^4) = \mathrm{O}(s^4)$$

$$\frac{r^2}{\ell^2}\mathrm{O}(s^8) = [\mathrm{O}(1)]^2\,\mathrm{O}(s^8) = \mathrm{O}(s^8)$$

Because both r and ℓ are "big" quantities, their ratio is roughly one, and we simply write O(1) for the ratio. Because the order terms $\mathrm{O}(s^4)$ and $\mathrm{O}(s^8)$ are also of order higher than three, they are left in the order form. To represent all these order terms that have an order higher than three, we simply write $\mathrm{O}(s^4)$ in Equation 3.6, since the practice is to let the lowest order term represent the presence of higher order terms that may follow. We have taken the time to demonstrate how order terms are handled because this technique is frequently used in this chapter.

We now substitute Equation 3.6 into Equation 3.5 and rearrange to obtain (remember $\ell < 0$, so $-\ell$ is positive)

$$T = -\ell\sqrt{1+x} \tag{3.7a}$$

where

$$x = \left(\frac{1}{\ell} - \frac{1}{r}\right)\frac{R^2}{\ell} - 2\sin\phi\frac{Rh}{\ell^2} + \frac{h^2}{\ell^2} + \mathrm{O}(s^4) \tag{3.7b}$$

Our next task is to find expressions for the direction cosines α, β, γ in terms of R, h, and other quantities. One way to find the basic formulas for α, β, γ is to draw a box with T as the diagonal, as we show in Figure 3.3. By looking at the

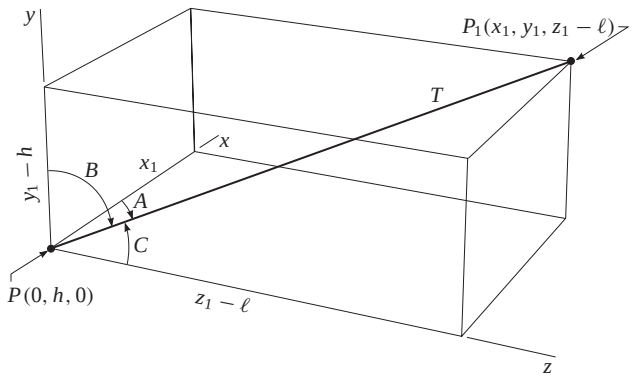

Figure 3.3

coordinates of P and P_1, we can determine the edge lengths of the box; namely x_1, $y_1 - h$, $z_1 - \ell$, respectively. By inspection of the box, we write the basic formula for α; then, replace x_1 by $R\cos\phi$ (see Figure 3.2), substitute Equation 3.7a, rewrite slightly, and use the binomial power series 3.1:

$$\begin{aligned}\alpha = \cos A = \frac{x_1}{T} &= \frac{R\cos\phi}{-\ell\sqrt{1+x}} \\ &= -\cos\phi\frac{R}{\ell}(1+x)^{-\frac{1}{2}} \\ &= -\cos\phi\frac{R}{\ell}\left[1 - \frac{1}{2}x + \mathrm{O}(x^2)\right]\end{aligned}$$

Finally, we replace x with Equation 3.7b and rearrange into terms of R, R^3, R^2h, Rh^2 and an order term of $\mathrm{O}(s^5)$—terms like these will appear frequently in our development of third-order theory:

$$\begin{aligned}\alpha = &-\cos\phi\frac{R}{\ell} + \frac{1}{2}\left(\frac{1}{\ell} - \frac{1}{r}\right)\cos\phi\frac{R^3}{\ell^2} \\ &- \sin\phi\cos\phi\frac{R^2h}{\ell^3} + \frac{1}{2}\cos\phi\frac{Rh^2}{\ell^3} + \mathrm{O}(s^5)\end{aligned} \tag{3.8}$$

Applying the same procedure we have just outlined for α, we obtain expressions for β and γ (see Figure 3.2 for y_1):

$$\begin{aligned}\beta = \cos B = \frac{y_1 - h}{T} &= \frac{R\sin\phi - h}{-\ell\sqrt{1+x}} \\ &= \left(-\sin\phi\frac{R}{\ell} + \frac{h}{\ell}\right)(1+x)^{-\frac{1}{2}} \\ &= \left(-\sin\phi\frac{R}{\ell} + \frac{h}{\ell}\right)\left[1 - \frac{1}{2}x + \mathrm{O}(x^2)\right)] \\ &= -\sin\phi\frac{R}{\ell} + \frac{h}{\ell} + \frac{1}{2}\left(\frac{1}{\ell} - \frac{1}{r}\right)\sin\phi\frac{R^3}{\ell^2} \\ &\quad - \left[\frac{1}{2}\left(\frac{1}{\ell} - \frac{1}{r}\right) + \frac{\sin^2\phi}{\ell}\right]\frac{R^2h}{\ell^2} \\ &\quad + \frac{3}{2}\sin\phi\frac{Rh^2}{\ell^3} - \frac{h^3}{2\ell^3} + \mathrm{O}(s^5)\end{aligned} \tag{3.9}$$

$$\begin{aligned}\gamma = \cos C = \frac{z_1 - \ell}{T} &= \frac{z_1 - \ell}{-\ell\sqrt{1+x}} \\ &= \left(-\frac{z_1}{\ell} + 1\right)(1+x)^{-\frac{1}{2}} \\ &= \left(-\frac{z_1}{\ell} + 1\right)\left[1 - \frac{1}{2}x + \mathrm{O}(x^2)\right] \\ &= 1 - \frac{R^2}{2\ell^2} + \sin\phi\frac{Rh}{\ell^2} - \frac{h^2}{2\ell^2} + \mathrm{O}(s^4)\end{aligned} \tag{3.10}$$

where in the derivation of γ we used Equation 3.4 to replace the z_1 that appears in the form $-z_1/\ell$.

Our next step is to obtain an expansion that represents the cosine of the angle of incidence θ; for convenience, we obtain an expression for $\cos^2\theta$. To obtain this expression, we use several of the equations we developed in Chapter 2. A good reference for the equations we need is the flow chart in Figure 2.19. Because we are working with only one surface, we drop the i subscripts that appear in those equations; also, we change the curvature c to the radius r (remember, $c = 1/r$). By inspection of Figure 3.2, we see that the ray begins at the point P where

$$x = 0,\ y = h,\ z = 0,\ t = -\ell \tag{3.11}$$

Substituting these values into Equation 2.22, we get

$$\begin{aligned} e &= t\gamma - (x\alpha + y\beta + z\gamma) \\ &= -\ell\gamma - h\beta \end{aligned} \tag{3.12}$$

We substitute the same values of Equation 3.11 into Equation 2.24, and then replace e with Equation 3.12:

$$\begin{aligned} M_z &= z + e\gamma - t \\ &= e\gamma + \ell \\ &= \ell - h\beta\gamma - \ell\gamma^2 \end{aligned} \tag{3.13}$$

Working in a similar way with Equation 2.29, we get

$$\begin{aligned} M^2 &= x^2 + y^2 + z^2 - e^2 + t^2 - 2tz \\ &= h^2 - e^2 + \ell^2 \\ &= \ell^2 + h^2 - h^2\beta^2 - 2\ell h\beta\gamma - \ell^2\gamma^2 \end{aligned} \tag{3.14}$$

Using Equation 2.35, squaring to remove the root for convenience, substituting Equations 3.13 and 3.14, and rearranging, we obtain

$$\begin{aligned} \cos^2\theta &= \gamma^2 - c(cM^2 - 2M_z) \\ &= \gamma^2 - \frac{1}{r}\left(\frac{1}{r}M^2 - 2M_z\right) \\ &= \frac{2\ell}{r} - \frac{\ell^2}{r^2} - \frac{h^2}{r^2} + \frac{h^2}{r^2}\beta^2 \\ &\qquad - \frac{2\ell}{r}\left(\frac{1}{\ell} - \frac{1}{r}\right)h\beta\gamma \\ &\qquad + \ell^2\left(\frac{1}{\ell} - \frac{1}{r}\right)^2\gamma^2 \end{aligned} \tag{3.15}$$

We now work with each of the terms that contain β or γ. We first note that the coefficient of β^2, namely h^2/r^2 is an $\mathrm{O}(s^2)$ term. Next, we mentally observe that when we square β in Equation 3.9, the lowest order terms are also $\mathrm{O}(s^2)$ terms. Thus,

$$\frac{h^2}{r^2}\beta^2 = \mathrm{O}(s^2)\,\mathrm{O}(s^2) = \mathrm{O}(s^4) \tag{3.16}$$

so it doesn't contribute to the third-order expansion of $\cos^2\theta$.

For the $\beta\gamma$ term, we observe that the coefficient has the following order property:

$$\begin{aligned} -\frac{2\ell}{r}\left(\frac{1}{\ell} - \frac{1}{r}\right)h &= -\frac{2\ell}{r}\left(\frac{h}{\ell} - \frac{h}{r}\right) \\ &= \mathrm{O}(1)\,\mathrm{O}(s) = \mathrm{O}(s) \end{aligned}$$

and, referring to Equations 3.9 and 3.10, that $\beta\gamma = \mathrm{O}(s)$. Therefore, we shall obtain terms that contribute to the third-order expansion when we perform the multiplication in detail:

$$\begin{aligned} &-\frac{2\ell}{r}\left(\frac{1}{\ell} - \frac{1}{r}\right)h\beta\gamma \\ &\qquad = \frac{2}{r}\left(\frac{1}{\ell} - \frac{1}{r}\right)\sin\phi\, Rh \\ &\qquad\qquad - \frac{2}{r}\left(\frac{1}{\ell} - \frac{1}{r}\right)h^2 + \mathrm{O}(s^4) \end{aligned} \tag{3.17}$$

Finally, we multiply out the last term in Equation 3.15, the γ^2 term given by Equation 3.10, and obtain:

$$\begin{aligned} &\ell^2\left(\frac{1}{\ell} - \frac{1}{r}\right)^2\gamma^2 \\ &\quad = \ell^2\left(\frac{1}{\ell} - \frac{1}{r}\right)^2 - \left(\frac{1}{\ell} - \frac{1}{r}\right)^2 R^2 \\ &\qquad + 2\left(\frac{1}{\ell} - \frac{1}{r}\right)^2\sin\phi\, Rh \\ &\qquad\qquad - \left(\frac{1}{\ell} - \frac{1}{r}\right)^2 h^2 + \mathrm{O}(s^4) \end{aligned} \tag{3.18}$$

We obtain the final expansion for $\cos^2\theta$ by substituting the preceding expansions given in Equations 3.16, 3.17, and 3.18 into Equation 3.15. Although we get a long expression at first, many terms cancel, so the final form is a much more manageable expression:

$$\begin{aligned} \cos^2\theta = 1 &- \left(\frac{1}{\ell} - \frac{1}{r}\right)^2 R^2 \\ &+ \frac{2}{\ell}\left(\frac{1}{\ell} - \frac{1}{r}\right)\sin\phi\, Rh \\ &- \frac{h^2}{\ell^2} + \mathrm{O}(s^4) \end{aligned} \tag{3.19}$$

We have now finished the expansion of the equations that relate to translation of the ray from the object point P to the point P_1 on the refracting surface of radius r—we have included the cosine squared of the angle of incidence θ with the translation equations. Next, we obtain the expansions of the refraction equations; these expansions correspond to the equations in the bottom half of the flow chart in Figure 2.19.

3.2.2 Power series for refraction

Referring to the flow chart in Figure 2.19, the equations we start with are Equations 2.45, 2.47, and 2.46. Continuing the simplified notation of this chapter, these equations are

$$\mu = \frac{n}{n'} \tag{3.20}$$

$$\cos\theta' = +\sqrt{1-\mu^2(1-\cos^2\theta)} \tag{3.21}$$

$$g = \cos\theta' - \mu\cos\theta \tag{3.22}$$

We obtained a power series for $\cos^2\theta$ in the previous section, which we named Equation 3.19. To get a power series for $\cos\theta$, we write

$$\cos^2\theta = 1 + x \tag{3.23a}$$

where

$$x = -\left(\frac{1}{\ell}-\frac{1}{r}\right)^2 R^2 + \frac{2}{\ell}\left(\frac{1}{\ell}-\frac{1}{r}\right)\sin\phi\, Rh - \frac{h^2}{\ell^2} + \mathrm{O}(s^4) \tag{3.23b}$$

We note that every term in the expression for x is a small term; therefore, x itself is small, and we can use the binomial power series of Equation 3.1 to write

$$\cos\theta = \sqrt{1+x} = (1+x)^{\frac{1}{2}} = 1 + \frac{1}{2}x + \mathrm{O}(x^2) \tag{3.24}$$

We use the preceding equations and the binomial power series in Equation 3.1 to derive

$$\begin{aligned} g &= \cos\theta' - \mu\cos\theta \\ &= +\sqrt{1-\mu^2(1-\cos^2\theta)} - \mu\cos\theta \\ &= +\sqrt{1-\mu^2(-x)} - \mu\sqrt{1+x} \\ &= \left(1+\mu^2 x\right)^{\frac{1}{2}} - \mu\left(1+x\right)^{\frac{1}{2}} \\ &= \left(1+\frac{1}{2}\mu^2 x\right) - \mu\left(1+\frac{1}{2}x\right) + \mathrm{O}(x^2) \end{aligned}$$

We now substitute Equation 3.23b for x and rearrange to get the power series for g

$$g = 1-\mu + \frac{\mu(1-\mu)}{2}\left(\frac{1}{\ell}-\frac{1}{r}\right)^2 R^2 - \frac{\mu(1-\mu)}{\ell}\left(\frac{1}{\ell}-\frac{1}{r}\right)\sin\phi\, Rh + \frac{\mu(1-\mu)}{2\ell^2}h^2 + \mathrm{O}(s^4) \tag{3.25}$$

A glance again at the flow chart in Figure 2.19 shows that after obtaining the power series for g we need the power series for α', β', and γ'. To get α' (remember $\alpha' = \cos A'$), we first copy its expression from Equation 2.52a, namely

$$\alpha' = \mu\alpha - cgx_1$$

From Figure 3.2, we have $x_1 = R\cos\phi$. As usual, we replace c by $1/r$. The power series for α and g are given by Equations 3.8 and 3.25, respectively. When we substitute all these expressions into α', we get such a long expression that it is easier to start a notation where we give names to the coefficients of R, h combinations; thus

$$\begin{aligned} \alpha' &= \mu\alpha - cgx_1 \\ &= \mu\alpha - \frac{1}{r}\,g\,R\cos\phi \\ &= a_1 R + a_2 R^3 + a_3 R^2 h + a_4 R h^2 + \mathrm{O}(s^5) \end{aligned} \tag{3.26}$$

where

$$a_1 = -\left[\frac{1}{r} + \mu\left(\frac{1}{\ell}-\frac{1}{r}\right)\right]\cos\phi \tag{3.27a}$$

$$a_2 = \frac{\mu}{2}\left(\frac{1}{\ell}-\frac{1}{r}\right)\left\{\frac{1}{\ell}\left(\frac{1}{\ell}-\frac{1}{r}\right) + \frac{1}{r}\left[\frac{1}{r}+\mu\left(\frac{1}{\ell}-\frac{1}{r}\right)\right]\right\}\cos\phi \tag{3.27b}$$

$$a_3 = -\frac{\mu}{\ell}\left\{\frac{1}{\ell}\left(\frac{1}{\ell}-\frac{1}{r}\right) + \frac{1}{r}\left[\frac{1}{r}+\mu\left(\frac{1}{\ell}-\frac{1}{r}\right)\right]\right\}\sin\phi\cos\phi \tag{3.27c}$$

$$a_4 = \frac{\mu}{2\ell^2}\left[\left(\frac{1}{\ell}-\frac{1}{r}\right)+\frac{\mu}{r}\right]\cos\phi \tag{3.27d}$$

Working out these expressions requires patience, and they may look rather intimidating. However, we should keep in mind that many of these expressions will simplify when we finally translate to the paraxial plane. In the end, we do obtain all the equations that describe the third-order aberrations.

Proceeding in a similar way, we note from Figure 3.2 that $y_1 = R\sin\phi$, and starting with Equation 2.52b, which represents $\beta' = \cos B'$, we get

$$\begin{aligned} \beta' &= \mu\beta - cgy_1 \\ &= \mu\beta - \frac{1}{r}\,g\,R\sin\phi \\ &= b_1 R + b_2 h \\ &\quad + b_3 R^3 + b_4 R^2 h + b_5 R h^2 + b_6 h^3 + \mathrm{O}(s^5) \end{aligned} \tag{3.28}$$

where

$$b_1 = -\left[\frac{1}{r} + \mu\left(\frac{1}{\ell} - \frac{1}{r}\right)\right]\sin\phi \tag{3.29a}$$

$$b_2 = \frac{\mu}{\ell} \tag{3.29b}$$

$$b_3 = \frac{\mu}{2}\left(\frac{1}{\ell} - \frac{1}{r}\right)\left\{\frac{1}{\ell}\left(\frac{1}{\ell} - \frac{1}{r}\right) + \frac{1}{r}\left[\frac{1}{r} + \mu\left(\frac{1}{\ell} - \frac{1}{r}\right)\right]\right\}\sin\phi \tag{3.29c}$$

$$b_4 = -\frac{\mu}{2\ell^2}\left(\frac{1}{\ell} - \frac{1}{r}\right) - \frac{\mu}{\ell}\left\{\frac{1}{\ell}\left(\frac{1}{\ell} - \frac{1}{r}\right) + \frac{1}{r}\left[\frac{1}{r} + \mu\left(\frac{1}{\ell} - \frac{1}{r}\right)\right]\right\}\sin^2\phi \tag{3.29d}$$

$$b_5 = \frac{\mu}{2\ell^2}\left[\left(\frac{3}{\ell} - \frac{1}{r}\right) + \frac{\mu}{r}\right]\sin\phi \tag{3.29e}$$

$$b_6 = -\frac{\mu}{2\ell^3} \tag{3.29f}$$

The expression for $\gamma' = \cos C'$, which is given by Equation 2.52c, has an extra term in it when compared to α' and β':

$$\gamma' = \mu\gamma - cgz_1 + g$$

We substitute Equation 3.10 for γ, Equation 3.25 for g, Equation 3.4 for z_1, and replace c by $1/r$:

$$\begin{aligned}\gamma' &= \mu\gamma - cgz_1 + g \\ &= \mu\gamma - \frac{1}{r}gz_1 + g \\ &= 1 - c_1R^2 - c_2Rh - c_3h^2\end{aligned} \tag{3.30}$$

where

$$c_1 = \frac{1}{2}\left[\frac{1}{r} + \mu\left(\frac{1}{\ell} - \frac{1}{r}\right)\right]^2 \tag{3.31a}$$

$$c_2 = -\frac{\mu}{\ell}\left[\frac{1}{r} + \mu\left(\frac{1}{\ell} - \frac{1}{r}\right)\right]\sin\phi \tag{3.32b}$$

$$c_3 = \frac{\mu^2}{2\ell^2} \tag{3.32c}$$

Thus, we have obtained the power series for the primed direction cosines α', β', γ' that describe refraction at the surface of radius r. We now want to obtain the equations for translation to the paraxial image plane—first, we shall translate to an arbitrary image plane, and then make it the paraxial image plane.

3.2.3 Translation to an image plane

We have obtained power series for $\alpha' = \cos A'$, $\beta' = \cos B'$, and $\gamma' = \cos C'$, which means that we have described the direction of the ray after refraction at the surface of radius r. We next trace the ray forward to an image plane a distance ℓ' from the vertex V, this vertex is the new origin for coordinate system, as we diagram in Figure 3.4. In this section, we view ℓ' as arbitrary, which means that the placement of the image plane is not fixed. In terms of our new coordinate system, the coordinates of P_1 are (x_1, y_1, z_1), as shown in Figure 3.4. We have

$$\left.\begin{aligned} x_1 &= R\cos\phi, \\ y_1 &= R\sin\phi, \\ z_1 &= \frac{R^2}{2r} + r\mathrm{O}(s^4) \end{aligned}\right\} \tag{3.33}$$

where x_1, y_1 are obtained from Figure 3.2, and z_1 is given by Equation 3.4. The ray travels a distance T' to the point P' with coordinates (x', y', ℓ'), as shown in Figure 3.4.

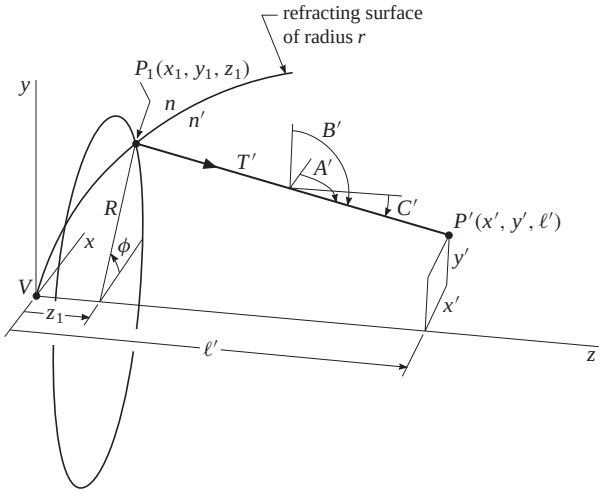

Figure 3.4

So that we can more easily see the relationships between T' and the direction cosines α', β', γ', we draw the diagram in Figure 3.5. We draw T' as the body diagonal in

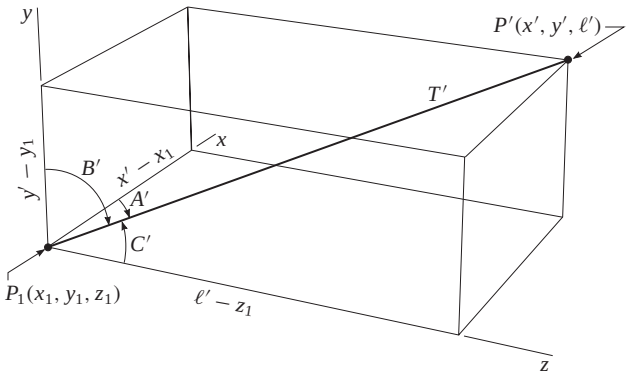

Figure 3.5

the box, and also incline T' upward, rather than downward as in Figure 3.4, to make it easier to read the relationships by inspection. We see that

$$\alpha' = \cos A' = \frac{x' - x_1}{T'} \tag{3.34a}$$

$$\beta' = \cos B' = \frac{y' - y_1}{T'} \tag{3.34b}$$

$$\gamma' = \cos C' = \frac{\ell' - z_1}{T'} \tag{3.34c}$$

We next solve Equation 3.34c for T' to get

$$T' = \frac{\ell' - z_1}{\gamma'} \tag{3.35}$$

Then we solve Equation 3.34a for x' and substitute for T' with Equation 3.35:

$$x' = x_1 + T'\alpha' = x_1 + \frac{(\ell' - z_1)\alpha'}{\gamma'} \tag{3.36}$$

and in a similar way

$$y' = y_1 + T'\beta' = y_1 + \frac{(\ell' - z_1)\beta'}{\gamma'} \tag{3.37}$$

To obtain the power series for x' in Equation 3.36, we use Equation 3.33 to substitute for x_1, Equation 3.4 for z_1, Equation 3.26 for α', and Equation 3.30 for γ'. Because our expression is so long, we use a distinctive format:

$$\begin{aligned} x' &= R\cos\phi \\ &\quad + \frac{\left[\ell' - \dfrac{R^2}{2r} - r\mathrm{O}(s^4)\right]\left[\begin{array}{r} a_1R + a_2R^3 \\ + a_3R^2h \\ + a_4Rh^2 \\ + \mathrm{O}(s^5) \end{array}\right]}{1 - x} \end{aligned} \tag{3.38a}$$

where

$$x = c_1R^2 + c_2Rh + c_3h^2 \tag{3.38b}$$

We use the $\gamma' = 1 - x$ format because γ' is in the denominator. To move it into the numerator, we recognize that x in Equation 3.38b is composed of three terms each of which is small, so x itself is small. Thus, we use the binomial expansion of Equation 3.1 to obtain

$$\begin{aligned} \frac{1}{\gamma'} = \frac{1}{1-x} &= (1-x)^{-1} = 1 + x + \mathrm{O}(x^2) \\ &= 1 + c_1R^2 + c_2Rh + c_3h^2 + \mathrm{O}(s^4) \end{aligned} \tag{3.39}$$

We replace the $1/(1-x)$ in Equation 3.38a with the expansion in Equation 3.39, and then multiply out all the expressions; we group together the terms involving R, R^3, R^2h, and Rh^2. This work is somewhat tedious; however, software programs like *Mathematica* make the task easier. We summarize the work below:

$$\begin{aligned} x' &= R\cos\phi \\ &\quad + \left[\ell' - \frac{R^2}{2r} - r\mathrm{O}(s^4)\right] \\ &\qquad \left[a_1R + a_2R^3 + a_3R^2h + a_4Rh^2 + \mathrm{O}(s^5)\right] \\ &\qquad \left[1 + c_1R^2 + c_2Rh + c_3h^2 + \mathrm{O}(s^4)\right] \\ &= \left(\ell' a_1 + \cos\phi\right) R && (3.40a) \\ &\quad + \left(\ell' a_2 + \ell' a_1 c_1 - \frac{a_1}{2r}\right) R^3 && (3.40b) \\ &\quad + \left(\ell' a_3 + \ell' a_1 c_2\right) R^2 h && (3.40c) \\ &\quad + \left(\ell' a_4 + \ell' a_1 c_3\right) Rh^2 && (3.40d) \\ &\quad + \ell'\mathrm{O}(s^5) \end{aligned}$$

In a similar way, we obtain a power series for y'—we get more terms in this expression because h lies in the yz plane. We start with Equation 3.37, replace y_1 and z_1 using Equations 3.33, β' by Equation 3.28, and $1/\gamma'$ by Equation 3.39:

$$\begin{aligned} y' &= R\sin\phi \\ &\quad + \left[\ell' - \frac{R^2}{2r} - r\mathrm{O}(s^4)\right] \\ &\qquad \left[b_1R + b_2h \right. \\ &\qquad\quad \left. + b_3R^3 + b_4R^2h + b_5Rh^2 + b_6h^3 + \mathrm{O}(s^5)\right] \\ &\qquad \left[1 + c_1R^2 + c_2Rh + c_3h^2 + \mathrm{O}(s^4)\right] \\ &= \left(\ell' b_1 + \sin\phi\right) R && (3.41a) \\ &\quad + \left(\ell' b_2\right) h && (3.41b) \\ &\quad + \left(\ell' b_3 + \ell' b_1 c_1 - \frac{b_1}{2r}\right) R^3 && (3.41c) \\ &\quad + \left(\ell' b_4 + \ell' b_1 c_2 + \ell' b_2 c_1 - \frac{b_2}{2r}\right) R^2 h && (3.41d) \\ &\quad + \left(\ell' b_5 + \ell' b_1 c_3 + \ell' b_2 c_2\right) Rh^2 && (3.41e) \\ &\quad + \left(\ell' b_6 + \ell' b_2 c_3\right) h^3 && (3.41f) \\ &\quad + \ell'\mathrm{O}(s^5) \end{aligned}$$

With Equations 3.40 and 3.41, we have acquired the desired power series for x' and y' through the third order in terms of R and h. In review, the quantities x', y' are the coordinates of a point P' on a plane a distance ℓ' from the vertex V of a refracting surface of radius r. This point $P'(x', y', \ell')$ marks the point a ray strikes on the image plane after traveling from an object point P through a refracting surface. We next investigate the meaning of Equations 3.40 and 3.41 relative to an image point on the paraxial plane.

3.3 The Paraxial Image Plane

For the object point $P(x, y)$ where

$$x = 0 \qquad y = h \tag{3.42a}$$

the ideal image location $P'_o(x', y')$—that is, the paraxial image point—is one for which

$$x' = 0 \qquad y' = h' \tag{3.42b}$$

true for any ray that passes through the refracting surface at any value of R or ϕ from the object point P for any value of h, as we diagram in Figure 3.6. When we look at the power

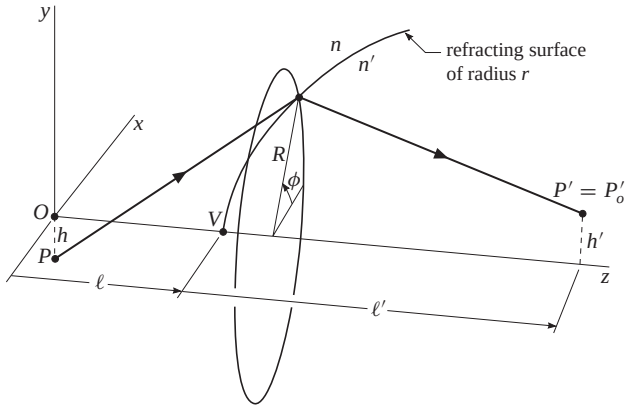

Figure 3.6

series for x' and y' in Equations 3.40 and 3.41, respectively, we see that the largest term is the R term in x', and both an R and h term in y'. We look at these terms first.

3.3.1 The image equations

In an attempt to make x' become zero in Equations 3.40, we start with the largest term, the R term in Equation 3.40a, which we set equal to zero:

$$(\ell' a_1 + \cos\phi)\, R = 0 \tag{3.43}$$

The idea for satisfying this equation is to find a suitable value for ℓ', which has no value yet. Choosing a value for ℓ' is equivalent to moving the image plane (on which P' rests) along the z axis until Equation 3.43 is true. Algebraically, we must have

$$\ell' a_1 + \cos\phi = 0 \tag{3.44}$$

We now obtain several important relations from this equation. First, we replace a_1 in Equation 3.44 by using Equation 3.27a:

$$\ell' \left\{ -\left[\frac{1}{r} + \mu \left(\frac{1}{\ell} - \frac{1}{r} \right) \right] \cos\phi \right\} + \cos\phi = 0$$

The $\cos\phi$ factors out, and we rearrange the expression that remains into

$$\mu \left(\frac{1}{\ell} - \frac{1}{r} \right) = \frac{1}{\ell'} - \frac{1}{r} \tag{3.45a}$$

We rearrange Equation 3.45a slightly to obtain

$$\frac{1}{r} + \mu \left(\frac{1}{\ell} - \frac{1}{r} \right) = \frac{1}{\ell'} \tag{3.45b}$$

and with a little more work,

$$\frac{1-\mu}{r} = \frac{1}{\ell'} - \frac{\mu}{\ell} \tag{3.45c}$$

To get an equation that is useful later, we multiply both sides of the previous equation by $(1/\ell - 1/r)$:

$$\left(\frac{1-\mu}{r} \right) \left(\frac{1}{\ell} - \frac{1}{r} \right) = \frac{1}{\ell'} \left(\frac{1}{\ell} - \frac{1}{r} \right) - \frac{\mu}{\ell} \left(\frac{1}{\ell} - \frac{1}{r} \right)$$

With the help of Equation 3.45a, this equation becomes

$$\left(\frac{1-\mu}{r} \right) \left(\frac{1}{\ell} - \frac{1}{r} \right) = \frac{1}{\ell'} \left(\frac{1}{\ell} - \frac{1}{r} \right) - \frac{1}{\ell} \left(\frac{1}{\ell'} - \frac{1}{r} \right) \tag{3.45d}$$

Finally, to get the most important equation of all, we substitute $\mu = n/n'$ (we defined μ in Equation 3.20) into Equation 3.45a, and obtain the object-image relation

$$-\frac{n}{\ell} + \frac{n'}{\ell'} = \frac{n' - n}{r} \tag{3.45e}$$

which agrees with Equation 1.135a in Example 1.5.4, where we discussed the paraxial properties of an optical system of one surface. Therefore, if we select ℓ' so that it satisfies any of Equations 3.45, we obtain the image plane position that is identical with the paraxial image plane of Chapter 1.

We observe that the y' power series in Equations 3.41 also has a term in R, namely Equation 3.41a. When we set this equation to zero, we get

$$\left(\ell' b_1 + \sin\phi \right) R = 0 \tag{3.46}$$

which implies that

$$\ell' b_1 + \sin\phi = 0$$

Substituting Equation 3.29a for b_1, we have

$$\ell' \left\{ -\left[\frac{1}{r} + \mu \left(\frac{1}{\ell} - \frac{1}{r} \right) \right] \sin\phi \right\} + \sin\phi = 0$$

In this equation the $\sin\phi$ terms factors out, and we obtain

$$\mu \left(\frac{1}{\ell} - \frac{1}{r} \right) = \frac{1}{\ell'} - \frac{1}{r}$$

which is identical to Equation 3.45a; that is, we get the same result as before.

3.3.2 The image height h'

According to Equations 3.42, when $y = h$, we have $y' = h'$ for the ideal image; therefore, we expect that the h term in Equation 3.41b equals h':

$$h' = (\ell' b_2)h = \ell' \frac{\mu}{\ell} h = \frac{n\ell'}{n'\ell} h \tag{3.47}$$

where we have substituted Equation 3.29b for b_2 and replaced μ by n/n' (see Equation 3.20). Thus, the transverse magnification m_T is

$$m_T = \frac{y'}{y} = \frac{h'}{h} = \frac{n\ell'}{n'\ell} \tag{3.48}$$

which agrees with the m_T given by Equation 1.135b in Example 1.5.4.

3.3.3 The x' and y' equations on the paraxial plane

We rewrite the power series on the paraxial plane for x' and y' as given in Equations 3.40 and 3.41 using what we have learned in the previous two sections as embodied in Equations 3.43, 3.46, and 3.47:

$$x' = \left(\ell' a_2 + \ell' a_1 c_1 - \frac{a_1}{2r}\right) R^3 \tag{3.49a}$$

$$+ \left(\ell' a_3 + \ell' a_1 c_2\right) R^2 h \tag{3.49b}$$

$$+ \left(\ell' a_4 + \ell' a_1 c_3\right) R h^2 \tag{3.49c}$$

$$+ \ell' \mathrm{O}(s^5)$$

and

$$y' = h' \tag{3.50a}$$

$$+ \left(\ell' b_3 + \ell' b_1 c_1 - \frac{b_1}{2r}\right) R^3 \tag{3.50b}$$

$$+ \left(\ell' b_4 + \ell' b_1 c_2 + \ell' b_2 c_1 - \frac{b_2}{2r}\right) R^2 h \tag{3.50c}$$

$$+ \left(\ell' b_5 + \ell' b_1 c_3 + \ell' b_2 c_2\right) R h^2 \tag{3.50d}$$

$$+ \left(\ell' b_6 + \ell' b_2 c_3\right) h^3 \tag{3.50e}$$

$$+ \ell' \mathrm{O}(s^5)$$

The a's, b's, and c's that appear in these equations also become simpler on the paraxial plane. When we substitute Equation 3.45b into Equations 3.27, we get

$$a_1 = -\frac{\cos\phi}{\ell'} \tag{3.51a}$$

$$a_2 = \frac{\mu}{2}\left(\frac{1}{\ell} - \frac{1}{r}\right)\left[\frac{1}{\ell}\left(\frac{1}{\ell} - \frac{1}{r}\right) + \frac{1}{\ell' r}\right]\cos\phi \tag{3.51b}$$

$$a_3 = -\frac{\mu}{\ell}\left[\frac{1}{\ell}\left(\frac{1}{\ell} - \frac{1}{r}\right) + \frac{1}{\ell' r}\right]\sin\phi\cos\phi \tag{3.51c}$$

$$a_4 = \frac{\mu}{2\ell^2}\left[\left(\frac{1}{\ell} - \frac{1}{r}\right) + \frac{\mu}{r}\right]\cos\phi \tag{3.51d}$$

and we have obtained the simpler equations for the a's. We perform the same operation for the b's in Equations 3.29; substituting Equation 3.45b, we have

$$b_1 = -\frac{\sin\phi}{\ell'} \tag{3.52a}$$

$$b_2 = \frac{\mu}{\ell} \tag{3.52b}$$

$$b_3 = \frac{\mu}{2}\left(\frac{1}{\ell} - \frac{1}{r}\right)\left[\frac{1}{\ell}\left(\frac{1}{\ell} - \frac{1}{r}\right) + \frac{1}{\ell' r}\right]\sin\phi \tag{3.52c}$$

$$b_4 = -\frac{\mu}{2\ell^2}\left(\frac{1}{\ell} - \frac{1}{r}\right) - \frac{\mu}{\ell}\left[\frac{1}{\ell}\left(\frac{1}{\ell} - \frac{1}{r}\right) + \frac{1}{\ell' r}\right]\sin^2\phi \tag{3.52d}$$

$$b_5 = \frac{\mu}{2\ell^2}\left[\left(\frac{3}{\ell} - \frac{1}{r}\right) + \frac{\mu}{r}\right]\sin\phi \tag{3.52e}$$

$$b_6 = -\frac{\mu}{2\ell^3} \tag{3.52f}$$

Substituting Equation 3.45b for the c's in Equations 3.31:

$$c_1 = \frac{1}{2\ell'^2} \tag{3.53a}$$

$$c_2 = -\frac{\mu}{\ell\ell'}\sin\phi \tag{3.53b}$$

$$c_3 = \frac{\mu^2}{2\ell^2} \tag{3.53c}$$

3.4 The Five Third-Order Aberrations

As we stated in Equation 3.42b, and as Figure 3.6 shows, the ideal image location at P'_o is one with coordinates $x' = 0$ and $y' = h'$ on the paraxial plane, which means that ideally the coefficients of R^3, R^2h, Rh^2, and h^3 in Equations 3.49 and 3.50 should be zero. It turns out, however, that except for a few special cases, it is impossible to find zero values for all these coefficients at the same time. In general, all we can do is make these coefficients small. These terms involving R^3, R^2h, Rh^2, and h^3 make up the third-order aberrations, and we want to study the properties of each of these terms.

3.4.1 Spherical aberration

Spherical aberration is composed of the terms in R^3 in Equations 3.49 and 3.50. Because there is no h in these terms, spherical aberration is always present independent of where the object point P is; that is, P can be on axis or off axis, but spherical aberration is still present for all nonzero values of R and of the coefficients of R^3. We shall investigate the properties of spherical aberration by studying the behavior of P' on the paraxial plane as a function of R and ϕ.

We name the R^3 term, Expression 3.49a, with the symbol x'_{SA}; that is,

$$x'_{SA} = \left(\ell' a_2 + \ell' a_1 c_1 - \frac{a_1}{2r}\right) R^3 \tag{3.54}$$

Substituting Equations 3.51a, 3.51b, and 3.53a, we have after a little rearrangement

$$\begin{aligned} x'_{SA} &= \frac{1}{2}\left\{\ell'\mu\left(\frac{1}{\ell}-\frac{1}{r}\right)\left[\frac{1}{\ell}\left(\frac{1}{\ell}-\frac{1}{r}\right)+\frac{1}{\ell' r}\right]\right. \\ &\qquad \left. -\frac{1}{\ell'}\left(\frac{1}{\ell'}-\frac{1}{r}\right)\right\}\cos\phi\, R^3 \\ &= \frac{1}{2}\left[\ell'\frac{\mu}{\ell}\left(\frac{1}{\ell}-\frac{1}{r}\right)^2+\frac{1}{r}\mu\left(\frac{1}{\ell}-\frac{1}{r}\right)\right. \\ &\qquad \left. -\frac{1}{\ell'}\left(\frac{1}{\ell'}-\frac{1}{r}\right)\right]\cos\phi\, R^3 \end{aligned}$$

Then we replace $\mu(1/\ell - 1/r)$ with $(1/\ell' - 1/r)$ by Equation 3.45a, replace μ with n/n', and simplify:

$$\begin{aligned} x'_{SA} &= \frac{1}{2}\left[\ell'\frac{\mu}{\ell}\left(\frac{1}{\ell}-\frac{1}{r}\right)^2+\frac{1}{r}\left(\frac{1}{\ell'}-\frac{1}{r}\right)\right. \\ &\qquad \left. -\frac{1}{\ell'}\left(\frac{1}{\ell'}-\frac{1}{r}\right)\right]\cos\phi\, R^3 \\ &= -\frac{\ell'}{2n'}\left[-\frac{n}{\ell}\left(\frac{1}{\ell}-\frac{1}{r}\right)^2\right. \\ &\qquad \left. +\frac{n'}{\ell'}\left(\frac{1}{\ell'}-\frac{1}{r}\right)^2\right]\cos\phi\, R^3 \\ &= -D_{SA}\cos\phi\, R^3 \end{aligned} \tag{3.55}$$

where

$$D_{SA} = \frac{\ell'}{2n'}\left[-\frac{n}{\ell}\left(\frac{1}{\ell}-\frac{1}{r}\right)^2+\frac{n'}{\ell'}\left(\frac{1}{\ell'}-\frac{1}{r}\right)^2\right] \tag{3.56}$$

We write Equation 3.55 with a minus sign in front so that D_{SA} is positive for $\ell < 0$ and $\ell' > 0$.

Similarly, along the y' axis, we use Expression 3.50b:

$$y'_{SA} = \left(\ell' b_3 + \ell' b_1 c_1 - \frac{b_1}{2r}\right) R^3 \tag{3.57}$$

When we substitute Equations 3.52a, 3.52c, and 3.53a, we find the expression is identical with the one for x'_{SA} except $\cos\phi$ is replaced by $\sin\phi$:

$$y'_{SA} = -D_{SA}\sin\phi\, R^3 \tag{3.58}$$

The path traced in the paraxial plane around the ideal image P'_o by x'_{SA} and y'_{SA} as a function of ϕ is a circle, as found by squaring the equations in Equations 3.55 and 3.58, adding, and then using a trig identity:

$$\begin{aligned} x'^2_{SA} + y'^2_{SA} &= (-D_{SA}\cos\phi\, R^3)^2 + (-D_{SA}\sin\phi\, R^3)^2 \\ &= (D_{SA}\, R^3)^2(\cos^2\phi + \sin^2\phi) \\ &= (D_{SA}\, R^3)^2 \\ &= R^2_{SA} \end{aligned} \tag{3.59}$$

where

$$R_{SA} = D_{SA}\, R^3 \tag{3.60}$$

is the radius of the circle. The situation is described by the diagram in Figure 3.7. The little arrows in the diagram show that as P_1 moves counterclockwise around the circle of radius R, the point P'_{SA} also moves counterclockwise on the spherical aberration circle of radius R_{SA}.

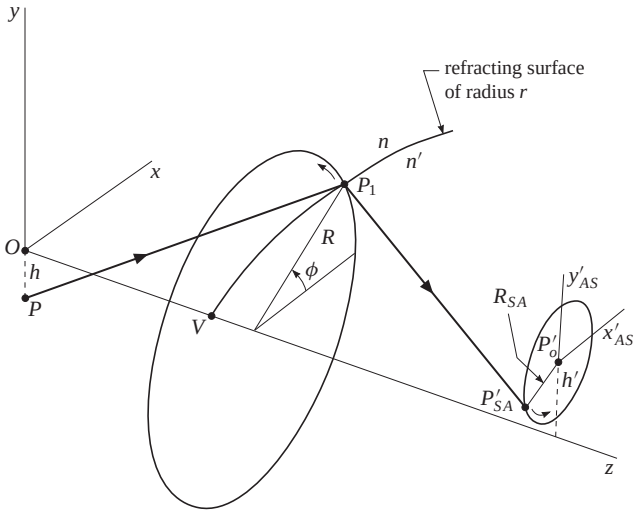

Figure 3.7 Spherical aberration: the ideal image point is P'_o and the point marking the image point produced by spherical aberration of third-order theory is P'_{SA}.

Example 3.4.1 Spherical aberration—third order versus exact. In Chapter 2 in Example 2.4.3, we worked with a single surface of $r = 20$ mm, and traced exactly several incident, parallel rays through the surface. In the diagram of that example, Figure 2.37, the ideal image point was the focal point F', and spherical aberration was measured by TSA. Our third-order theory of spherical aberration should approximate the results that we obtained in that example.

We first copy several of the numerical values from Example 2.4.3, namely: $r = 20$ mm, $n = 1$, $n' = 1.5$, and the object distance $\ell = -\infty$. We substitute these values into Equation 3.45e to calculate ℓ'; we find $\ell' = 60$ mm. Substituting now into Equation 3.56, we get

$$D_{SA} = 0.000555556\,\text{mm}^{-2}$$

Next, we use Equations 3.55 and 3.58; we see that we need values for ϕ and R. Comparing Figures 3.7 and 2.37, we see that $\phi = 90$ deg, that R plays the role of y, and to get precise correspondence, that $h = R$—however, what h is really does not matter in spherical aberration because h does not appear in the spherical aberration equations. Substituting $\phi = 90$ deg and the preceding value for D_{SA} into Equations 3.55 and 3.58, we obtain

$$x'_{SA} = -D_{SA} \cos\phi \, R^3 = 0$$
$$y'_{SA} = -D_{SA} \sin\phi \, R^3 = -\left(0.000555556\,\text{mm}^{-2}\right) R^3$$

We observe that the values for y'_{SA} should be in approximate agreement with the TSA values in Example 2.4.3. We list the exact values of TSA and the approximate y'_{SA} ones in the table in Figure 3.8. We see that the agreement is quite good.

R (mm)	TSA (mm)	y'_{SA} (mm)
0.	0.	0.
1.	−0.000556367	−0.000555556
2.	−0.00447055	−0.00444444
3.	−0.0151999	−0.015
4.	−0.0364084	−0.0355556
5.	−0.0720891	−0.0694444

Figure 3.8 Comparison of values: the TSA are the exact values of Example 2.4.3, and the y'_{SA} are the approximate ones calculated in this example.

To illustrate the good agreement between the exact TSA values (open circles) and the approximate y'_{SA} ones (solid circles), we draw the graph in Figure 3.9. The exact open circles begin to emerge only when R reaches 5 mm.

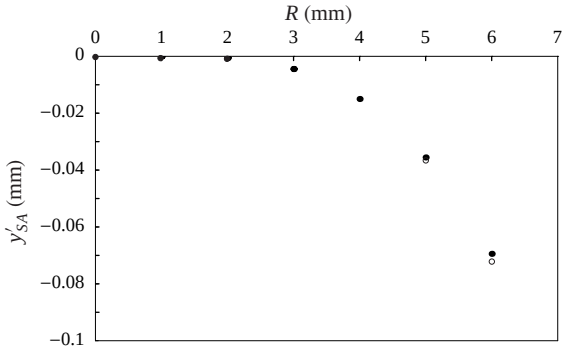

Figure 3.9 The solid circles are the approximate y'_{SA} values, and the open circles are the exact TSA values. The R on the horizontal axis is the same as the y in Example 2.4.3. The vertical axis is labeled y'_{SA} for simplicity; however, it represents TSA also.

We have finished our our work on the first of the third-order aberrations, spherical aberration. We now turn our attention to the next third-order aberration: coma.

3.4.2 Coma

Referring back to Equations 3.49 and 3.50, we see that the next terms to consider after the spherical aberration R^3 terms, are the R^2h terms; these terms describe the aberration called coma—sometimes considered the worst of the third-order aberrations. The derivation follows the same pattern as before in spherical aberration.

We copy Expression 3.49b and name it x'_{CM}; we then substitute Equations 3.51c, 3.51a, and 3.53b for a_3, a_1, and c_2, respectively:

$$\begin{aligned} x'_{CM} &= \left(\ell' a_3 + \ell' a_1 c_2\right) R^2 h \\ &= \left\{ -\ell' \frac{\mu}{\ell} \left[\frac{1}{\ell}\left(\frac{1}{\ell} - \frac{1}{r}\right) + \frac{1}{\ell' r} \right] \sin\phi\cos\phi \right. \\ &\qquad \left. + (-\cos\phi)\left(-\frac{\mu}{\ell\ell'}\sin\phi\right) \right\} R^2 h \end{aligned}$$

where one pair of ℓ' terms was canceled. We next factor out terms, replace μ by n/n', use Equation 3.47, and the trig identity of $\sin 2\phi = 2\sin\phi\cos\phi$ to obtain

$$\begin{aligned} x'_{CM} &= \left[-\frac{1}{\ell}\left(\frac{1}{\ell} - \frac{1}{r}\right) \right. \\ &\qquad \left. - \frac{1}{\ell' r} + \frac{1}{\ell'^2} \right] \frac{\mu \ell'}{\ell} \sin\phi\cos\phi R^2 h \\ &= -\left[\frac{1}{\ell}\left(\frac{1}{\ell} - \frac{1}{r}\right) \right. \\ &\qquad \left. - \frac{1}{\ell'}\left(\frac{1}{\ell'} - \frac{1}{r}\right) \right] \sin\phi\cos\phi R^2 \left(\frac{n\ell'}{n'\ell} h\right) \\ &= -\frac{1}{2}\left[\frac{1}{\ell}\left(\frac{1}{\ell} - \frac{1}{r}\right) \right. \\ &\qquad \left. - \frac{1}{\ell'}\left(\frac{1}{\ell'} - \frac{1}{r}\right) \right] \sin 2\phi R^2 h' \\ &= -D_{CM} \sin 2\phi R^2 h' \end{aligned} \tag{3.61}$$

where

$$D_{CM} = \frac{1}{2}\left[\frac{1}{\ell}\left(\frac{1}{\ell} - \frac{1}{r}\right) - \frac{1}{\ell'}\left(\frac{1}{\ell'} - \frac{1}{r}\right) \right] \tag{3.62}$$

We get the equation for y'_{CM} in a similar way. We start with Expression 3.50c, and name it y'_{CM}:

$$y'_{CM} = \left(\ell' b_4 + \ell' b_1 c_2 + \ell' b_2 c_1 - \frac{b_2}{2r} \right) R^2 h$$

We then substitute Equations 3.52a, 3.52b, 3.52d for the b's, Equations 3.53a, 3.53b for the c's, and use the trig identity of $2\sin^2\phi = 1 - \cos 2\phi$ to get after some manipulation

$$y'_{CM} = -D_{CM}\left(2 - \cos 2\phi\right) R^2 h' \tag{3.63}$$

where D_{CM} is given by Equation 3.62.

We now want to investigate the properties of coma by studying the equations that we have just derived:

$$x'_{CM} = -D_{CM} \sin 2\phi R^2 h' \tag{3.64a}$$

$$y'_{CM} = -D_{CM} (2 - \cos 2\phi) R^2 h' \tag{3.64b}$$

where

$$D_{CM} = \frac{1}{2}\left[\frac{1}{\ell}\left(\frac{1}{\ell} - \frac{1}{r}\right) - \frac{1}{\ell'}\left(\frac{1}{\ell'} - \frac{1}{r}\right)\right] \tag{3.64c}$$

We observe that when we write Equation 3.64b as

$$y'_{CM} + 2D_{CM} R^2 h' = D_{CM} \cos 2\phi R^2 h'$$

we can square it and Equation 3.64a, and then add to obtain

$$\begin{aligned} &x'^2_{CM} + \left(y'_{CM} + 2D_{CM} R^2 h'\right)^2 \\ &\quad = \left(D_{CM} \sin 2\phi R^2 h'\right)^2 + \left(D_{CM} \cos 2\phi R^2 h'\right)^2 \\ &\quad = \left(\sin^2 2\phi + \cos^2 2\phi\right)\left(D_{CM} R^2 h'\right)^2 \\ &\quad = \left(D_{CM} R^2 h'\right)^2 \end{aligned} \tag{3.65}$$

If we set

$$b' = 2D_{CM} R^2 h' \qquad r' = |D_{CM} R^2 h'| \tag{3.66}$$

then we can write Equation 3.65 more simply as

$$x'^2_{CM} + \left(y'_{CM} + b'\right)^2 = r'^2 \tag{3.67}$$

which we now recognize at the equation of a circle—the equation of a comatic circle—of radius r' with its center at $(0, -b')$, as we show in Figure 3.10. The reason we write r' as an absolute value in Equation 3.66 is because we want the radius of a circle to be positive—the term $D_{CM} R^2 h'$ can have negative values. The situation is simplest when $D_{CM} R^2 h' > 0$ for then b' is positive and $b' = 2r'$, which is the case in Figure 3.10.

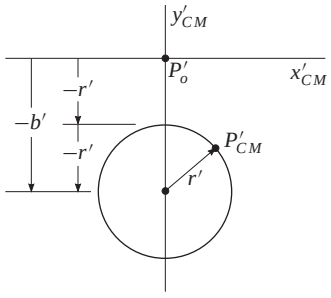

Figure 3.10 In this diagram, we assume $D_{CM} R^2 h' > 0$ so that $b' > 0$ and $b' = 2r'$. The point P'_o is the paraxial image point, and P'_{CM} is the image point due to coma.

Coma is the first of the third-order aberrations that depends on h' (or h), as well as R. We draw the travel of one ray in Figure 3.11.

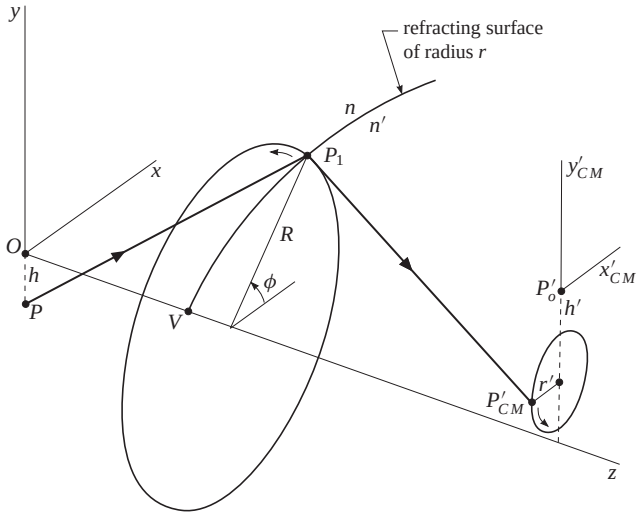

Figure 3.11 In this diagram, $\phi = 45$ deg.

An unusual aspect of coma is produced by the 2ϕ in Equations 3.64a and 3.64b. This property means that the image point P'_{CM} moves "twice as fast" around its image circle as the point P_1 does on the R circle. We use Figure 3.12 to show this behavior, where we should imagine that rays are drawn from P to the numbered points on the R circle, and from those points to the comatic-circle points with the same numbered points. We observe the "twice as fast" property, since going around once on the R circle causes a going around twice on the comatic circle.

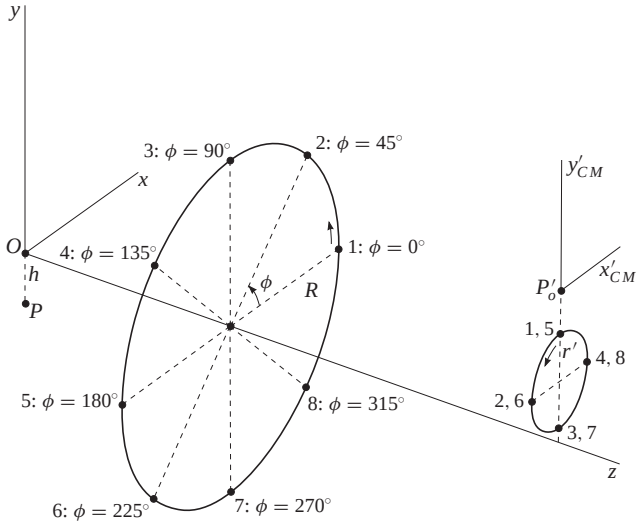

Figure 3.12 In this diagram, we understand that rays travel from P to the numbered points on the R circle, where they are refracted to pass through points with the same number on the comatic circle in the x'_{CM}, y'_{CM} plane.

Another important property of coma is brought out by the diagram in Figure 3.13, which is based on the equations for b' and r' in Equation 3.66, and the drawing in Figure 3.10.

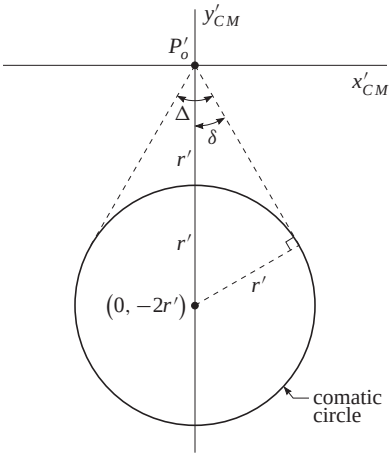

Figure 3.13

For convenience, just as in Figure 3.10, we have assumed that $D_{CM}R^2h' > 0$. By inspection of the right triangle, created by drawing a tangent line and a radius, we see that

$$\sin\delta = \frac{r'}{2r'} = \frac{1}{2}$$

$$\delta = 30\,\text{deg} \tag{3.68a}$$

and therefore, by symmetry,

$$\Delta = 60\,\text{deg} \tag{3.68b}$$

In fact, all the comatic circles that correspond to different values of R fit between the two tangent lines drawn in Figure 3.13. To illustrate this property, we look at a set of R circles and the comatic circles that result in the table of Figure 3.14. To help understand what we are doing, we look back at Figure 3.11 and observe a ray traveling from P to P_1 to P'_{CM} on the comatic circle. This ray is one of a cone of many rays that travel from P to points P_1 on the R circle—this cone of rays produces the comatic circle of radius r' in Figure 3.11. But in reality there are many other cones of rays traveling from P to points P_1 on circles that have radii bigger or smaller than R. In Figure 3.14, we look at a set of R circles that start with the radius R and then become smaller in increments of $R/4$. In the next two columns of the table, we calculate r' and b' for each of the comatic circles. Then we draw the comatic circles with their centers in Figure 3.15.

R	$r' = D_{CM}R^2h'$	$b' = 2r'$
R	r'	$2r'$
$\frac{3}{4}R$	$\frac{9}{16}r'$	$\frac{9}{8}r'$
$\frac{1}{2}R$	$\frac{1}{4}r'$	$\frac{1}{2}r'$
$\frac{1}{4}R$	$\frac{1}{16}r'$	$\frac{1}{8}r'$
0	0	0

Figure 3.14

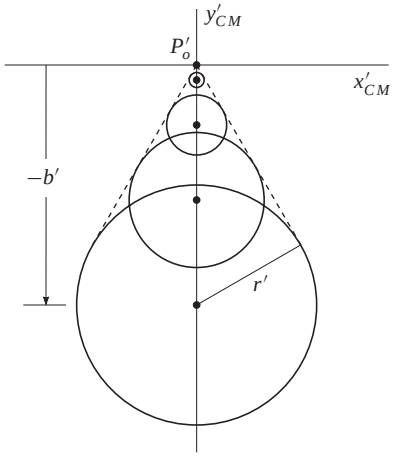

Figure 3.15

In three dimensions, the diagram for this situation is shown in Figure 3.16. The largest comatic circle in the x'_{CM}, y'_{CM} plane corresponds to the R circle, the next largest comatic circle corresponds to the $3R/4$ circle, and so on down to the smallest circles.

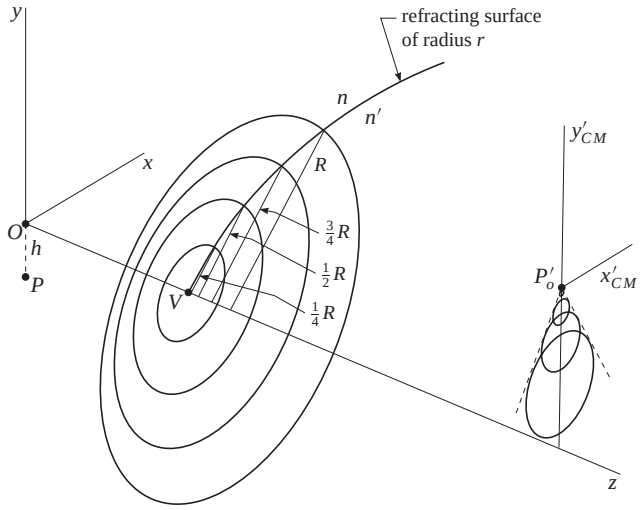

Figure 3.16

As Equations 3.64 show, coma also depends upon the image height h' (or the object height h). However, we are able to display the properties of coma by simply using the R circles, keeping h' fixed. For this reason, coma—and also spherical aberration—are called point aberrations. The next aberrations we study are astigmatism and curvature of field, which are both described by the Rh^2 expressions of Equations 3.49c and 3.50d. Astigmatism is another point aberration ($h' =$ constant), but not curvature of field (h' varies).

3.4.3 Astigmatism

Astigmatism and curvature of field are basically described by the same equations: in astigmatism we hold h' constant (the subject of this section), and in curvature of field, h' varies. We shall use the subscript AC to stand for both astigmatism and curvature of field.

We start with Expression 3.49c and substitute for a_1, a_4, and c_3 with Equations 3.51a, 3.51d, and 3.53c, respectively:

$$\begin{aligned} x'_{AC} &= \left(\ell' a_4 + \ell' a_1 c_3\right) Rh^2 \\ &= \left\{ \ell' \frac{\mu}{2\ell^2} \left[\left(\frac{1}{\ell} - \frac{1}{r} \right) + \frac{\mu}{r} \right] \cos\phi \right. \\ &\qquad \left. + \ell' \left(-\frac{\cos\phi}{\ell'} \right) \left(\frac{\mu^2}{2\ell^2} \right) \right\} Rh^2 \end{aligned}$$

We replace μ by n/n' (see Equation 3.20), factor out $\cos\phi$, ℓ^2, ℓ'^2, n^2/n'^2, $1/2$, and rearrange to get

$$\begin{aligned} x'_{AC} &= \frac{1}{2} \left\{ \frac{n'}{n\ell'} \left[\left(\frac{1}{\ell} - \frac{1}{r} \right) + \frac{n}{n'r} \right] \right. \\ &\qquad \left. - \left(\frac{1}{\ell'^2} \right) \right\} \cos\phi \, R \left(\frac{n\ell'}{n'\ell} h \right)^2 \\ &= -\frac{n'}{2\ell'} \left[-\frac{1}{n} \left(\frac{1}{\ell} - \frac{1}{r} \right) + \frac{1}{n'} \left(\frac{1}{\ell'} - \frac{1}{r} \right) \right] \cos\phi \, Rh'^2 \\ &= -D_{CR} \cos\phi \, Rh'^2 \end{aligned} \tag{3.69}$$

where the subscript CR stands for curvature of field and

$$D_{CR} = \frac{n'}{2\ell'} \left[-\frac{1}{n} \left(\frac{1}{\ell} - \frac{1}{r} \right) + \frac{1}{n'} \left(\frac{1}{\ell'} - \frac{1}{r} \right) \right] \tag{3.70}$$

We work in a similar way to obtain y_{AC}, except our expressions are somewhat longer. Into Expression 3.50d, we substitute for the b's and c's from Equations 3.52 and 3.53, and simplify as we did with x'_{AC} before:

$$\begin{aligned} y'_{AC} &= \left(\ell' b_5 + \ell' b_1 c_3 + \ell' b_2 c_2\right) Rh^2 \\ &= \left\{ \ell' \frac{\mu}{2\ell^2} \left[\left(\frac{3}{\ell} - \frac{1}{r} \right) + \frac{\mu}{r} \right] \sin\phi \right. \\ &\qquad + \ell' \left(-\frac{\sin\phi}{\ell'} \right) \left(\frac{\mu^2}{2\ell^2} \right) \\ &\qquad \left. + \ell' \left(\frac{\mu}{\ell} \right) \left(-\frac{\mu}{\ell\ell'} \sin\phi \right) \right\} Rh^2 \\ &= -\frac{n'}{2\ell'} \left[-\frac{1}{n} \left(\frac{3}{\ell} - \frac{1}{r} \right) \right. \\ &\qquad \left. + \frac{1}{n'} \left(\frac{3}{\ell'} - \frac{1}{r} \right) \right] \sin\phi \, Rh'^2 \end{aligned}$$

Although this expression has a convenient form, the terms $3/\ell$ and $3/\ell'$ cause a problem when we compare this expression with the one in Equation 3.70. Thus, to get an expression that contains the one in Equation 3.70, we expand the terms inside the brackets, and rearrange:

$$\begin{aligned} y'_{AC} &= -\frac{n'}{2\ell'} \left[-\frac{2}{n\ell} - \frac{1}{n\ell} + \frac{1}{nr} \right. \\ &\qquad \left. + \frac{2}{n'\ell'} + \frac{1}{n'\ell'} - \frac{1}{n'r} \right] \sin\phi \, Rh'^2 \\ &= -\frac{n'}{2\ell'} \left[2 \left(-\frac{1}{n\ell} + \frac{1}{n'\ell'} \right) \right. \\ &\qquad \left. - \frac{1}{n} \left(\frac{1}{\ell} - \frac{1}{r} \right) + \frac{1}{n'} \left(\frac{1}{\ell'} - \frac{1}{r} \right) \right] \sin\phi \, Rh'^2 \\ &= -\left\{ \frac{n'}{\ell'} \left(-\frac{1}{n\ell} + \frac{1}{n'\ell'} \right) \right. \\ &\qquad + \frac{n'}{2\ell'} \left[-\frac{1}{n} \left(\frac{1}{\ell} - \frac{1}{r} \right) \right. \\ &\qquad \left. \left. + \frac{1}{n'} \left(\frac{1}{\ell'} - \frac{1}{r} \right) \right] \right\} \sin\phi \, Rh'^2 \\ &= -\left(D_{AT} + D_{CR}\right) \sin\phi \, Rh'^2 \end{aligned} \tag{3.71}$$

where

$$D_{AT} = \frac{n'}{\ell'} \left(-\frac{1}{n\ell} + \frac{1}{n'\ell'} \right) \tag{3.72}$$

and D_{CR} is given by Equation 3.70. As we shall see at the end of this section, the D_{AT} expression relates to astigmatism, and the D_{CR} expression to curvature of field.

To make our analysis of the properties of astigmatism and curvature of field more convenient, we define two more quantities, D_1 and D_2. Going back to Equations 3.69 and 3.71, we write

$$x'_{AC} = -D_1 R \cos\phi \tag{3.73a}$$

$$y'_{AC} = -D_2 R \sin\phi \tag{3.73b}$$

where

$$D_1 = D_{CR} h'^2 \tag{3.74a}$$

$$D_2 = \left(D_{AT} + D_{CR}\right) h'^2 \tag{3.74b}$$

The path traced out on the paraxial image plane is given by the preceding equations for x'_{AC} and y'_{AC}. However, to investigate the properties of astigmatism and curvature of field, we need to describe not only what the ray does on the paraxial image plane according to the x'_{AC}, y'_{AC} coordinates, but extend the ray to another plane (called the image plane) parallel to the paraxial image plane, where we shall call the intersection point $\bar{P}$. To see all the features that are needed

to perform this description, we draw Figure 3.17; it is important to note that the coordinates of the points of importance—namely, P_1, P', $\bar{P}$—have their coordinates referenced to a coordinate system with origin at the paraxial image point P'_o. The ray is refracted at P_1 and then travels in a straight line first to the point P' on the paraxial image plane, and second to the point $\bar{P}$ on the image plane. The distance from P_1 to P' is T', and from P' to $\bar{P}$ the distance is $\bar{T}$.

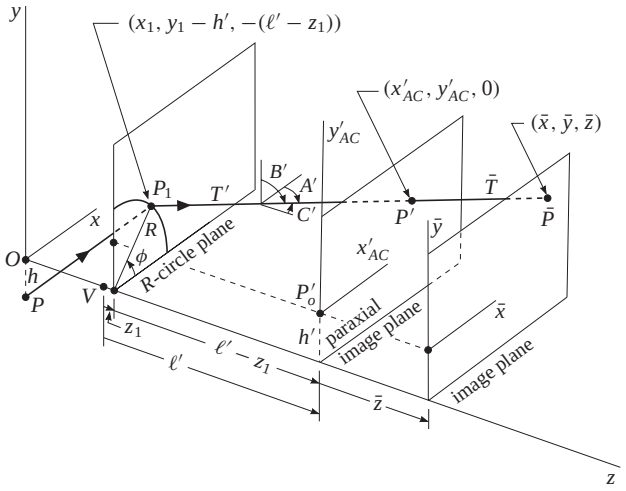

Figure 3.17 The points P_1, P', $\bar{P}$ have coordinates referenced to the paraxial image point P'_o.

To find expressions for the direction cosines α', β', γ', we draw the diagrams in Figures 3.18 to 3.20. In Figure 3.18, we show the projections of T' and $\bar{T}$ along the x axis, and we read by inspection,

$$\alpha' = \cos A' = \frac{x'_{AC} - x_1}{T'} = \frac{\bar{x} - x'_{AC}}{\bar{T}} \tag{3.75}$$

from which we obtain

$$\frac{\bar{T}}{T'} = \frac{\bar{x} - x'_{AC}}{x'_{AC} - x_1} \tag{3.76}$$

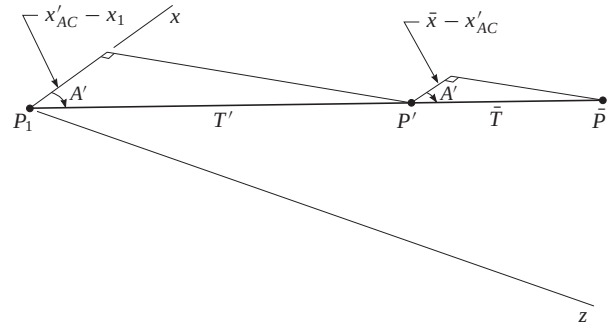

Figure 3.18

In a similar way, we draw the projections of T' and $\bar{T}$ along the y axis in Figure 3.19, and obtain

$$\beta' = \cos B' = \frac{y'_{AC} - (y_1 - h')}{T'} = \frac{\bar{y} - y'_{AC}}{\bar{T}} \tag{3.77}$$

which leads to

$$\frac{\bar{T}}{T'} = \frac{\bar{y} - y'_{AC}}{y'_{AC} - (y_1 - h')} \tag{3.78}$$

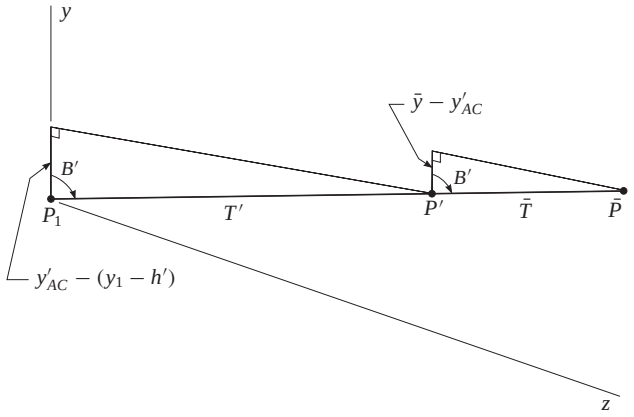

Figure 3.19

And finally, using Figure 3.20 to show the projections along the z axis, we have

$$\gamma' = \cos C' = \frac{\ell' - z_1}{T'} = \frac{\bar{z}}{\bar{T}} \tag{3.79}$$

and then

$$\frac{\bar{T}}{T'} = \frac{\bar{z}}{\ell' - z_1} \tag{3.80}$$

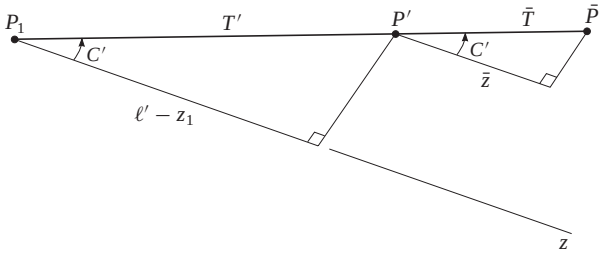

Figure 3.20

We now observe that we have three different expressions for $\bar{T}/T'$. We combine them in pairs; first, from Equations 3.76 and 3.80:

$$\frac{\bar{T}}{T'} = \frac{\bar{x} - x'_{AC}}{x'_{AC} - x_1} = \frac{\bar{z}}{\ell' - z_1} \tag{3.81}$$

We use the righthand two expressions in Equation 3.81, and solve for $\bar{x} - x'_{AC}$:

$$\bar{x} - x'_{AC} = \frac{x'_{AC} - x_1}{\ell' - z_1}\,\bar{z}$$

We solve this equation for $\bar{x}$, and invoke the condition that $\ell' >> z_1$ (which is the normally the case—see Figure 3.17):

$$\bar{x} = x'_{AC} + \frac{x'_{AC} - x_1}{\ell'}\,\bar{z} \tag{3.82}$$

In a similar way, we pair up Equations 3.78 and 3.80 to get

$$\frac{\bar{T}}{T'} = \frac{\bar{y} - y'_{AC}}{y'_{AC} - (y_1 - h')} = \frac{\bar{z}}{\ell' - z_1} \tag{3.83}$$

from which we have (using again, $\ell' >> z_1$)

$$\bar{y} - y'_{AC} = \frac{y'_{AC} - (y_1 - h')}{\ell'}\,\bar{z}$$

and then

$$\begin{aligned}\bar{y} &= y'_{AC} + \frac{y'_{AC} - (y_1 - h')}{\ell'}\,\bar{z} \\ &= y'_{AC} + \frac{y'_{AC} - y_1}{\ell'}\,\bar{z} + \frac{h'}{\ell'}\,\bar{z}\end{aligned} \tag{3.84}$$

In Equations 3.82 and 3.84, we first replace x_1 and y_1 by $R\cos\phi$ and $R\sin\phi$, respectively, using Equations 3.33; second, substitute for x'_{AC} and y'_{AC} with Equations 3.73; and third, use the inequalities $|D_1| << 1$ and $|D_2| << 1$ (which are normally true in third-order theory):

$$\bar{x} = -R\left(D_1 + \frac{\bar{z}}{\ell'}\right)\cos\phi \tag{3.85a}$$

$$\bar{y} = -R\left(D_2 + \frac{\bar{z}}{\ell'}\right)\sin\phi + \frac{h'}{\ell'}\,\bar{z} \tag{3.85b}$$

We rearrange each of these equations to place the negative of the trig function on the righthand side:

$$\frac{\bar{x}}{R\left(D_1 + \dfrac{\bar{z}}{\ell'}\right)} = -\cos\phi \tag{3.86a}$$

$$\frac{\bar{y} - \dfrac{h'}{\ell'}\bar{z}}{R\left(D_2 + \dfrac{\bar{z}}{\ell'}\right)} = -\sin\phi \tag{3.86b}$$

We square both sides of each of these equations, add, and use a trig identity to obtain the equation of an ellipse, namely

$$\frac{\bar{x}^2}{R^2\left(D_1 + \dfrac{\bar{z}}{\ell'}\right)^2} + \frac{\left(\bar{y} - h'\dfrac{\bar{z}}{\ell'}\right)^2}{R^2\left(D_2 + \dfrac{\bar{z}}{\ell'}\right)^2} = \cos^2\phi + \sin^2\phi = 1 \tag{3.87}$$

To make it easier to read this equation as one of an ellipse, we introduce several new quantities so that we can write

$$\frac{\bar{x}^2}{a^2} + \frac{(\bar{y} - k_2)^2}{b^2} = 1 \tag{3.88}$$

where

$$k_2 = h'\frac{\bar{z}}{\ell'} \tag{3.89a}$$

$$a = R\left(D_1 + \frac{\bar{z}}{\ell'}\right) \tag{3.89b}$$

$$b = R\left(D_2 + \frac{\bar{z}}{\ell'}\right) \tag{3.89c}$$

It is advantageous to briefly review the properties of an ellipse. The equation of the ellipse shown in Figure 3.21 is

$$\frac{(\bar{x} - k_1)^2}{a^2} + \frac{(\bar{y} - k_2)^2}{b^2} = 1 \tag{3.90}$$

where the coordinates (k_1, k_2) denote the center of the ellipse, a is the semimajor axis, and b is the semiminor axis. There are three special cases of interest that we can understand with the help of Figure 3.21; namely

1) $a = 0$: vertical straight line segment with
$$k_2 - b \le \bar{y} \le k_2 + b$$
2) $b = 0$: horizontal straight line segment with
$$k_1 - a \le \bar{x} \le k_1 + a$$
3) $a = \pm b$: circle with center at (k_1, k_2) and radius $|a|$.

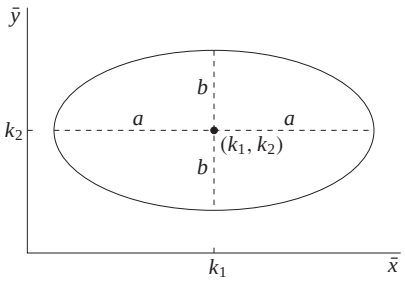

Figure 3.21

We make use of these properties of an ellipse to analyze astigmatism. First of all, when we look at Equation 3.88, we see that $k_1 = 0$ so the center of the astigmatism ellipse is always on the $\bar{y}$ axis. However, $k_2 = (h'/\ell')\bar{z}$ by Equation 3.89a, which implies that the center moves up and down the $\bar{y}$ axis as the value of $\bar{z}$ changes (see Figure 3.17). Continuing to look at Figure 3.17, we see that when $\bar{z} = 0$, then $k_2 = 0$ and the center of the ellipse is at P'_o—remember the origin of the $\bar{x}, \bar{y}$ axes is a distance h' above the z axis, just like P'_o.

Condition 1) $a = 0$**.** According to this condition, we get a straight line segment on the $\bar{y}$ axis; that is, a line image. We start with Equation 3.89b to get

$$a = R\left(D_1 + \frac{\bar{z}}{\ell'}\right) = 0$$

which yields

$$\bar{z} = \bar{z}_s = -\ell' D_1 = -\ell' D_{CR} h'^2 \tag{3.91}$$

where in the last step, we used Equation 3.74a. The s stands for sagittal, denoting a plane that is perpendicular to the meridional plane (or tangential plane; that is, the yz plane). To get the $\bar{x}, \bar{y}$ equations, we substitute Equation 3.91 and Equations 3.74 into Equations 3.85; we obtain

$$\bar{x} = 0 \tag{3.92a}$$

$$\bar{y} = -D_{AT} R h'^2 \sin\phi - D_{CR} h'^3 \tag{3.92b}$$

To construct the path $\bar{x}, \bar{y}$ traces out, we build the table in Figure 3.22, and then use it to draw the diagram in Figure 3.23, where we assume that $D_{CR} > 0$ and $D_{AT} > 0$. The path obtained is the line image on the $\bar{y}$ axis with center k_2 below the $\bar{x}, \bar{y}$ origin, and shifted $\bar{z}_s$ to the left of the paraxial plane (marked by P'_o, and the $\bar{x}, \bar{y}$ axes). The line segment is called a sagittal line image because the two rays that intersect at the same point in the line image lie in the sagittal plane (these are the rays for which $\phi = 0$ deg and $\phi = 180$ deg). As we mentioned before, the sagittal plane is perpendicular to the meridional plane, the yz plane. To make a simpler diagram, we did not draw the rays from the point P to the R circle.

$\bar{x} = 0$
$k_1 = 0$
$k_2 = -D_{CR} h'^3$

ϕ (deg)	$\bar{y}$
0	$-D_{CR} h'^3$
90	$-D_{AT} R h'^2 - D_{CR} h'^3$
180	$-D_{CR} h'^3$
270	$D_{AT} R h'^2 - D_{CR} h'^3$
360	$-D_{CR} h'^3$

Figure 3.22

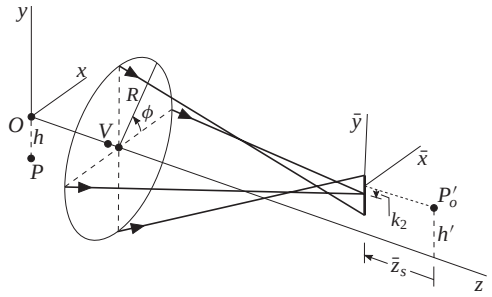

Figure 3.23 The sagittal line image.

Condition 2) $b = 0$**.** Under this condition we get another line image, but this time it is parallel to the $\bar{x}$ axis. Because $b = 0$, we start with Equation 3.89c to get

$$b = R\left(D_2 + \frac{\bar{z}}{\ell'}\right) = 0$$

which yields

$$\bar{z} = \bar{z}_t = -\ell' D_2 = -\ell' (D_{AT} + D_{CR}) h'^2 \tag{3.93}$$

where in the last step, we used Equation 3.74b. The t stands for tangential, another name for the meridional plane; that is, the yz plane. Proceeding as we did before, we obtain the $\bar{x}, \bar{y}$ equations by substituting Equation 3.93 and Equations 3.74 into Equations 3.85:

$$\bar{x} = D_{AT} R h'^2 \cos\phi \tag{3.94a}$$

$$\bar{y} = -(D_{AT} + D_{CR}) h'^3 \tag{3.94b}$$

Again we construct a table, and display it in Figure 3.24. We graph the information in the table in Figure 3.25, assuming that $D_{CR} > 0$ and $D_{AT} > 0$. As we expected, we get a line image parallel to the $\bar{x}$ axis (as well as the x axis). This line image is called a tangential line image because the two rays that meet at the same point (at $\bar{x} = 0$) are in the tangential plane—these two rays are the ones for which $\phi = 90$ deg and $\phi = 270$ deg, respectively.

$\bar{y} = -(D_{AT} + D_{CR}) h'^3$
$k_1 = 0$
$k_2 = \bar{y}$
$\quad = -(D_{AT} + D_{CR}) h'^3$

ϕ (deg)	$\bar{x}$
0	$D_{AT} R h'^2$
90	0
180	$-D_{AT} R h'^2$
270	0
360	$D_{AT} R h'^2$

Figure 3.24

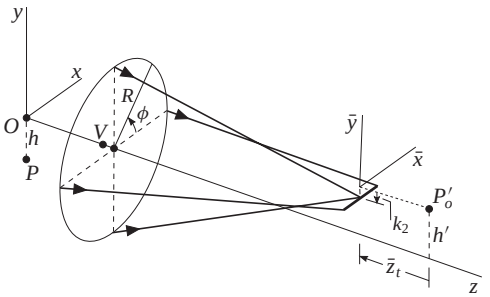

Figure 3.25 The tangential line image.

Condition 3) $a = \pm b$**.** From Figure 3.21 (and as stated above that diagram), we see that $a = \pm b$ gives a circle of radius $|a|$. Substituting Equation 3.89b and 3.89c, respectively, for a and b, and solving for $\bar{z}$, we find that only $a = -b$ yields a usable solution:

$$R\left(D_1 + \frac{\bar{z}}{\ell'}\right) = -R\left(D_2 + \frac{\bar{z}}{\ell'}\right)$$

$$\begin{aligned}\bar{z} = \bar{z}_c &= -\frac{\ell'}{2}(D_1 + D_2) \\ &= -\frac{\ell'}{2}(D_{AT} + 2D_{CR})\,h'^2 \end{aligned} \tag{3.95}$$

where we have substituted Equations 3.74 in the last step.

The value of $\bar{z}_c$ is located midway between the values of $\bar{z}_s$ and $\bar{z}_t$, as we can easily see by the following calculation:

$$\frac{1}{2}(\bar{z}_s + \bar{z}_t) = -\frac{\ell'}{2}(D_{AT} + 2D_{CR})\,h'^2 = z_c \tag{3.96}$$

where we have substituted Equations 3.91 and 3.93 for $\bar{z}_s$ and $\bar{z}_t$, respectively. We find the radius $|a|$ of the circle by using Equation 3.89b and substituting Equation 3.95 and Equations 3.74:

$$|a| = R\left|D_1 + \frac{\bar{z}}{\ell'}\right| = \frac{1}{2}|D_{AT}|\,Rh'^2 \tag{3.97}$$

We get the $\bar{x}$, $\bar{y}$ equations by substituting Equation 3.95 and Equations 3.74 into Equations 3.85:

$$\bar{x} = \frac{1}{2}D_{AT}Rh'^2\cos\phi \tag{3.98a}$$

$$\begin{aligned}\bar{y} &= -\frac{1}{2}D_{AT}Rh'^2\sin\phi - \frac{1}{2}(D_{AT} + 2D_{CR})\,h'^3 \\ &= -\frac{1}{2}D_{AT}Rh'^2\sin\phi + k_2 \end{aligned} \tag{3.98b}$$

where k_2 is found by substituting first Equation 3.95 into Equation 3.89a, and then using Equations 3.74:

$$\begin{aligned}k_2 = h'\frac{\bar{z}_c}{\ell'} &= -\frac{h'}{2}(D_1 + D_2) \\ &= -\frac{1}{2}(D_{AT} + 2D_{CR})h'^3 \end{aligned} \tag{3.99}$$

We build the table in Figure 3.26 with the help of Equations 3.98 and then draw the corresponding diagram of the circle image in Figure 3.27 (for $D_{AT} > 0$ and $D_{CR} > 0$).

ϕ (deg)	$\bar{x}$	$\bar{y}$
0	$\frac{1}{2}D_{AT}Rh'^2$	$+k_2$
90	0	$-\frac{1}{2}D_{AT}Rh'^2 + k_2$
180	$-\frac{1}{2}D_{AT}Rh'^2$	$+k_2$
270	0	$\frac{1}{2}D_{AT}Rh'^2 + k_2$
360	$\frac{1}{2}D_{AT}Rh'^2$	$+k_2$

Figure 3.26

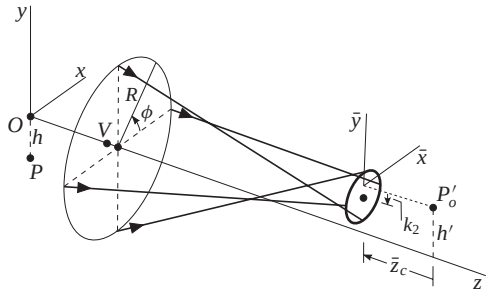

Figure 3.27 The circle image.

Summary. We summarize the images that we have described in the preceding discussion in Figure 3.28; we include the elliptical image in the paraxial image plane, where $\bar{z} = 0$ to give the center at P'_o where $k_1 = 0$, $k_2 = 0$ (see Equation 3.89a). An elliptical path is the usual image that is obtained on other planes than the special ones shown.

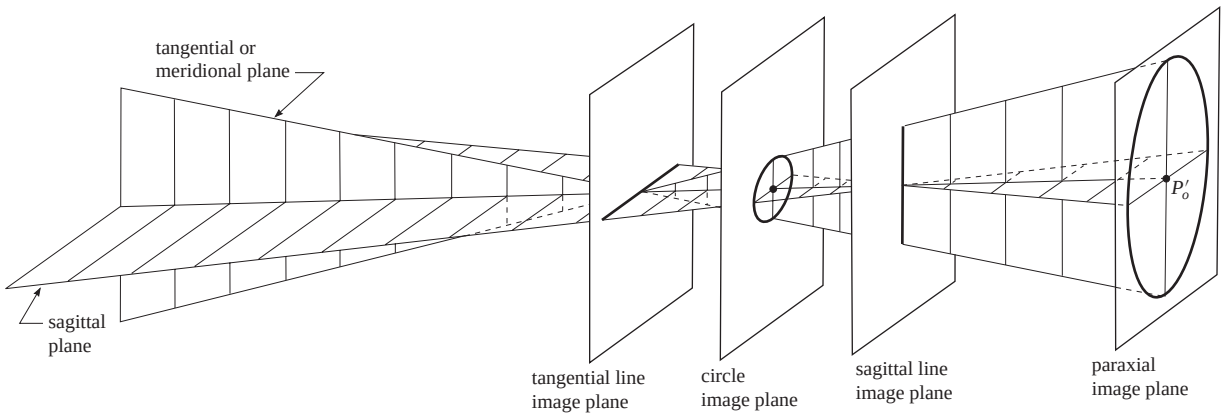

Figure 3.28 A diagram to illustrate the images on several important planes in astigmatism ($D_{AT} > 0$ and $D_{CR} > 0$). On other planes, the paths traced out are ellipses, somewhat like the ellipse on the paraxial image plane.

It is interesting to see what happens when we allow D_{AT} to tend to zero. To help us in this analysis, we summarize the important expressions of Equations 3.88 and 3.89 with D_1 and D_2 replaced by Equations 3.74:

$$\frac{\bar{x}^2}{a^2} + \frac{(\bar{y} - k_2)^2}{b^2} = 1 \tag{3.100}$$

where

$$k_2 = h' \frac{\bar{z}}{\ell'} \tag{3.101a}$$

$$a = R\left(D_{CR}h'^2 + \frac{\bar{z}}{\ell'}\right) \tag{3.101b}$$

$$b = R\left(D_{AT}h'^2 + D_{CR}h'^2 + \frac{\bar{z}}{\ell'}\right) \tag{3.101c}$$

Referring to Figure 3.21 and the conditions above that diagram, we can make our description more precise with the help of Equations 3.101 and the discussion on the previous pages; namely (assume, for convenience, $D_{AT} > 0$ and $D_{CR} > 0$):

1) sagittal line image: a vertical line segment with
$$a = 0 \quad \text{when} \quad \bar{z} = \bar{z}_s = -\ell' D_{CR} h'^2$$
endpoints given by
$$k_2 \pm b = \pm D_{AT} R h'^2 - D_{CR} h'^3$$
with $k_2 = -D_{CR}h'^3$, and length
$$(k_2 + b) - (k_2 - b) = 2D_{AT} R h'^2$$

2) tangential line image: a horizontal line segment with
$$b = 0 \quad \text{when} \quad \bar{z} = \bar{z}_t = -\ell' D_{AT} h'^2 - \ell' D_{CR} h'^2$$
endpoints given by (remember $k_1 = 0$)
$$k_1 \pm a = \mp D_{AT} R h'^2$$
and $k_2 = -D_{AT}h'^3 - D_{CR}h'^3$, and length
$$(k_2 - a) - (k_2 + a) = 2D_{AT} R h'^2$$

3) circle located at
$$\bar{z} = \bar{z}_c = -\frac{\ell'}{2} D_{AT} h'^2 - \ell' D_{CR} h'^2$$
with center at
$$k_1 = 0, \qquad k_2 = -\frac{1}{2} D_{AT} h'^3 - D_{CR} h'^3$$
and diameter
$$2|a| = D_{AT} R h'^2$$

Now let D_{AT} tend to zero. We observe from 1) that the position $\bar{z}_s$ and the center given by k_2 of the sagittal line image does not change; also that the $\bar{z}$ positions in the three conditions all become equal to $\bar{z}_s$, namely,

$$\bar{z}_t = \bar{z}_c = \bar{z}_s = -\ell' D_{CR} h'^2$$

In Equations 3.101b and 3.101c, the quantities a and b become equal implying that the usual elliptical paths become circles (as long as $a \neq 0$ and $b \neq 0$). What used to be the single circle in 3) becomes a point, since the radius $|a|$ goes to zero as $D_{AT} \to 0$. Also, the endpoints of both line images in 1) and 2) move toward their respective centers to a point located at the position of $\bar{y} = -D_{CR}h'^3$, the same as the k_2 center of the sagittal line image. Thus, to make a mental movie of the behavior of the images as $D_{AT} \to 0$, the elliptical paths all tend to circles; the line images get shorter, the circle at $\bar{z}_c$ gets smaller, all finally becoming points at the same point at the $\bar{z}$ position of the sagittal line image, $\bar{z}_s = -\ell' D_{CR} h'^2$, which doesn't move. Therefore, when $D_{AT} = 0$, the basic features of astigmatism disappear. Because D_{AT} has this property, we assigned this quantity the subscript $_{AT}$ to mean that it has the fundamental control over astigmatism.

3.4.4 Curvature of field

All three of the aberrations we have discussed—spherical aberration, coma, and astigmatism—are called point aberrations because their essential characteristics emerge for a fixed object point (h = constant, or what is the same, a fixed image point of h' = constant). To discuss the last two aberrations, curvature of field and distortion, we must move the object point, which in turn moves the image point.

For curvature of field, all the equations of the previous section still hold, but h and h' are no longer held constant. We note that most of these equations have terms of either h'^2 or h'^3, which means that curvature of field has a nonlinear behavior with h'. We assume, as usual, $D_{AT} > 0$ and $D_{CR} > 0$. To shorten our description, we will simply investigate what happens to the $\bar{z}$ positions of the line images and the circle; these are given by Equations 3.91, 3.93, and 3.95:

$$\bar{z}_s = -\ell' D_{CR} h'^2 \tag{3.102a}$$

$$\bar{z}_t = -\ell' \left(D_{AT} + D_{CR}\right) h'^2 \tag{3.102b}$$

$$\bar{z}_c = -\frac{\ell'}{2} \left(D_{AT} + 2D_{CR}\right) h'^2 \tag{3.102c}$$

To obtain numerical coefficients of h'^2, we assume that $n = 1$, $n' = 1.5$, $r = 100$ mm, $\ell = -300$ mm, and $\ell' = 900$ mm. We substitute these values first into Equation 3.72 to get $D_{AT} = 6.79012 \times 10^{-6}\,\text{mm}^{-2}$, then into Equation 3.70 to obtain $D_{CR} = 6.17284 \times 10^{-6}\,\text{mm}^{-2}$, and finally into Equations 3.102 to get

$$\bar{z}_s = \left(-0.00555556\,\text{mm}^{-1}\right) h'^2$$
$$\bar{z}_t = \left(-0.0116667\,\text{mm}^{-1}\right) h'^2$$
$$\bar{z}_c = \left(-0.00861111\,\text{mm}^{-1}\right) h'^2$$

We graph these equations in Figure 3.29.

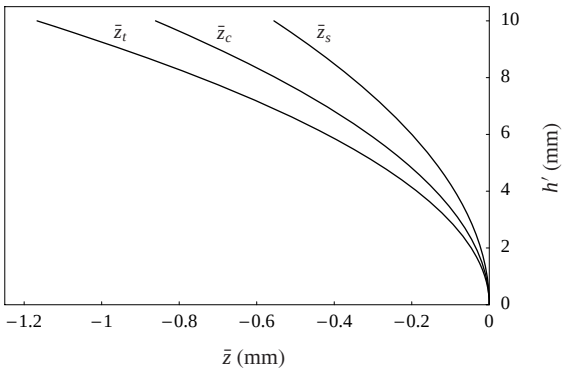

Figure 3.29

3.4.5 Distortion

The last third-order aberration is distortion, which is comprised of terms with h^3 present; it is the one aberration that has no R quantity. Looking back at Equations 3.49 and 3.50, we see that the x' equation has no h^3 term present, only the y' equation does, and so

$$x'_{DS} = 0 \tag{3.103}$$

$$y'_{DS} = \left(\ell' b_6 + \ell' b_2 c_3\right) h^3 \tag{3.104}$$

Substituting Equations 3.52f, 3.52b, and 3.53c for b_6, b_2, and c_3, respectively, Equation 3.104 becomes

$$\begin{aligned} y'_{DS} &= -\frac{1}{2}\left(\frac{n'}{\ell'}\right)^2 \left(\frac{1}{n^2} - \frac{1}{n'^2}\right) h'^3 \\ &= -D_{DS} h'^3 \end{aligned} \tag{3.105}$$

where

$$D_{DS} = \frac{1}{2}\left(\frac{n'}{\ell'}\right)^2 \left(\frac{1}{n^2} - \frac{1}{n'^2}\right) \tag{3.106}$$

with the help of $\mu = n/n'$; we also invoked Equation 3.47 to introduce the h' term.

In our description of distortion, it proves helpful to include the quantity h', (see Equation 3.50a); we also drop the DS subscript in the x' and y' terms to simplify our notation. Thus, we write

$$x' = x'_{DS} = 0 \tag{3.107}$$

$$y' = h' - D_{DS} h'^3 \tag{3.108}$$

It may be disturbing not to have a subscript of some kind for the x' and y' terms, but we do it in the interest of streamlining the fair amount of algebraic work we must perform.

To describe distortion, we must not only make the object point P move along the y axis, but we must also move it laterally parallel to the x and y axes; that is, we must work with object points that are anywhere on the xy plane, the object plane, as illustrated in Figure 3.30. The image is formed on the paraxial image plane, as shown by the x', y' axes in Figure 3.30. Both h and w are negative in this diagram.

However, an object point that moves in this way presents a problem because our equations, namely Equations 3.107 and 3.108, only work with a point P on the y axis. To make these equations describe the more general situation, we must rotate the coordinate axes through an angle ζ, as we show in Figures 3.31 and 3.32. In Figure 3.31 the rotated axes are named $\bar{x}$, $\bar{y}$, and the object point P is on the negative $\bar{y}$ axis a distance $\bar{h}$ away from O; the negative axis is where we have been placing P, although in distortion we shall move P almost anywhere on the object plane. In general, the $\bar{x}$, $\bar{y}$ axes are rotated until P is on either the negative or positive $\bar{y}$ axis. The corresponding situation on the paraxial image plane is shown in Figure 3.32, where the rotated axes are named the $\bar{x}'$, $\bar{y}'$ axes, and are rotated through the same angle ζ. In terms of the optical system we have been considering in this chapter, if the object point P is on the negative $\bar{y}$ axis, then the paraxial image point P'_o and the image point P' produced by distortion are on the positive $\bar{y}'$ axis (because there is no R or ϕ dependence in distortion). As we indicate in Figure 3.32, the paraxial image height of P'_o is $\bar{h}'$ from the origin O'. In this diagram, the coordinates of P'_o and P' are given in terms of the $\bar{x}'$, $\bar{y}'$ axes as $(0, \bar{h}')$ and $(0, \bar{y}')$, respectively.

By a rotation of axes we have presented a mechanism that allows the use of Equations 3.107 and 3.108 even when

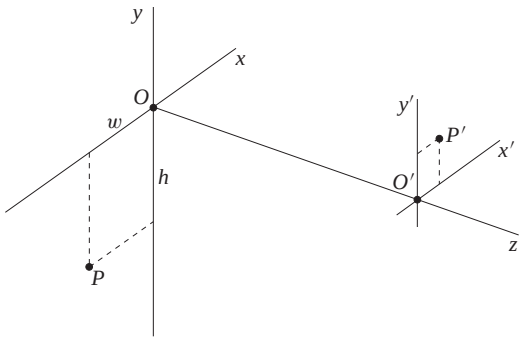

Figure 3.30 The object plane and paraxial image plane.

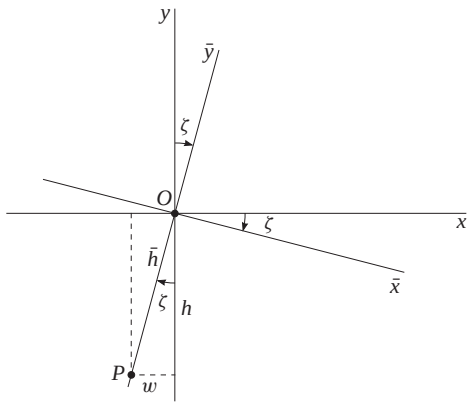

Figure 3.31 The object plane.

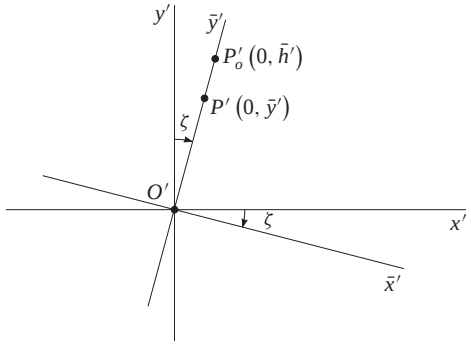

Figure 3.32 The paraxial image plane.

the object point P is not on the y axis. All we have to do is replace x', y', h, h' by $\bar{x}'$, $\bar{y}'$, $\bar{h}$, $\bar{h}'$, respectively; thus, Equations 3.107 and 3.108 become

$$\bar{x}' = 0 \tag{3.109}$$

$$\bar{y}' = \bar{h}' - D_{DS}\bar{h}'^3 \tag{3.110}$$

The coefficient D_{DS} remains the same because when we check Equation 3.106 we do not see any of the terms in the x', y', h, h' list. By Equation 3.47, we get in the rotated frame

$$\bar{h}' = \frac{n\ell'}{n'\ell}\bar{h} \tag{3.111}$$

By inspection of the object plane in Figure 3.31, we obtain the equations to calculate $\bar{h}$, $\sin\zeta$, $\cos\zeta$:

$$\bar{h} = \pm\sqrt{h^2 + w^2} \tag{3.112a}$$

$$\sin\zeta = \frac{w}{\bar{h}} \tag{3.112b}$$

$$\cos\zeta = \frac{h}{\bar{h}} \tag{3.112c}$$

To obtain x', y' in terms of $\bar{x}'$, $\bar{y}'$, we use the diagrams shown in Figures 3.33 and 3.34. The key point in these diagrams is

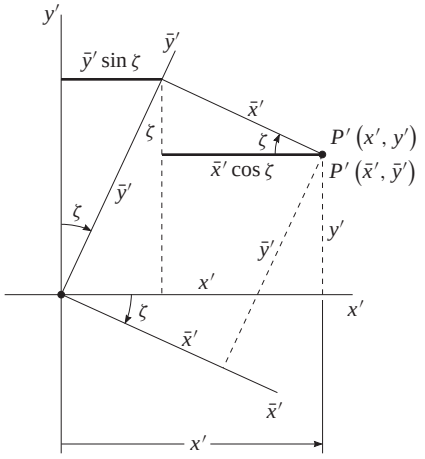

Figure 3.33 To obtain x' in terms of $\bar{x}'$, $\bar{y}'$.

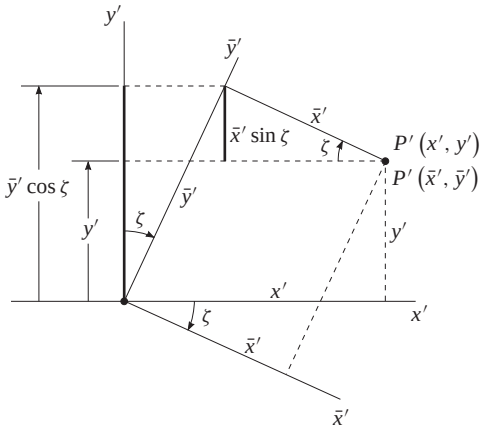

Figure 3.34 To obtain y' in terms of $\bar{x}'$, $\bar{y}'$.

the point P'; this point has coordinates x', y' in the primed coordinate system, and coordinates $\bar{x}'$, $\bar{y}'$ in the bar-primed coordinate system (the rotated axes). From Figure 3.33, we see that

$$x' = \bar{x}'\cos\zeta + \bar{y}'\sin\zeta \tag{3.113a}$$

and from Figure 3.34

$$y' = -\bar{x}'\sin\zeta + \bar{y}'\cos\zeta \tag{3.113b}$$

But Figure 3.32 shows that $\bar{x}' = 0$; therefore, Equations 3.113 become more simply

$$x' = \bar{y}'\sin\zeta \tag{3.114a}$$

$$y' = \bar{y}'\cos\zeta \tag{3.114b}$$

We now would like to draw graphs that display the properties of distortion. If we choose $n = 1$, $n' = 1.5$, $r = 5$ mm, and $\ell = -15$ mm, then Equation 3.45e says that $\ell' = 45$ mm. Substituting these values into Equations 3.106 and 3.111, we calculate

$$D_{DS} = 0.000308642\,\text{mm}^{-2} \tag{3.115a}$$

$$\bar{h}' = -2\,\bar{h} \tag{3.115b}$$

We use these values in the flow chart (which summarizes the equations we developed) in Figure 3.35 to graph distortion.

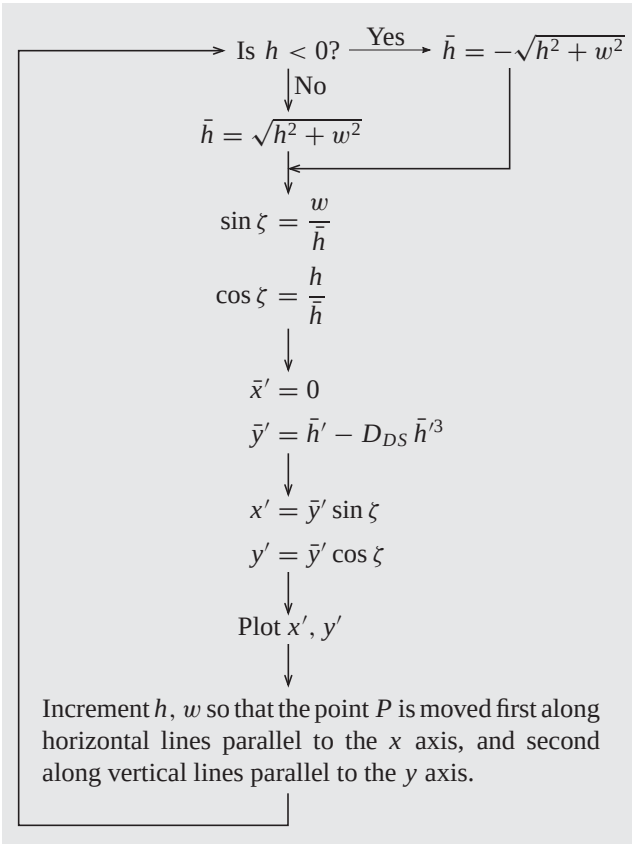

Figure 3.35 Flow chart for the calculation of distortion.

We show in Figure 3.36 the grid of lines in the object plane that the point P of Figure 3.30 moves along, horizontally from $w = -10\,\text{mm}$ to $w = 10\,\text{mm}$, and vertically from $h = -10\,\text{mm}$ to $h = 10\,\text{mm}$.

For each w, h pair of coordinates for the point P, the flow chart in Figure 3.35 is executed, and the x', y' coordinates of the point P' are calculated. The lines P' traces out are shown in Figure 3.37; the diagram is called barrel distortion because it reminds one of the way a barrel looks.

If we change the value of D_{DS} in Equation 3.115a to a negative one, namely

$$D_{DS} = -0.000308642\,\text{mm}^{-2}$$

then the distortion diagram we obtain is shown in Figure 3.38, where the shape reminds us of a pincushion.

Distortion is removed in an optical system by a symmetrical arrangement of lenses about a central stop (a stop is an aperture that limits the rays that pass through an optical system). What happens is that if the first lens causes barrel distortion, then the second lens causes pincushion distortion, and the two distortions cancel each other.

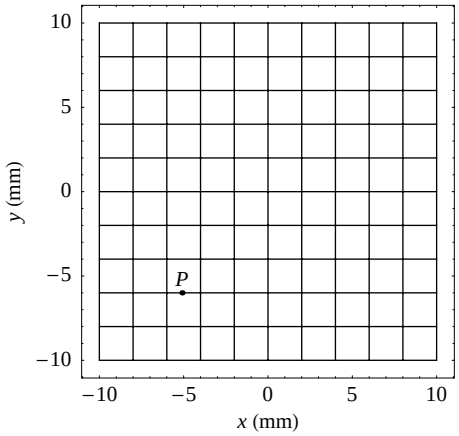

Figure 3.36 Grid of lines in the object plane.

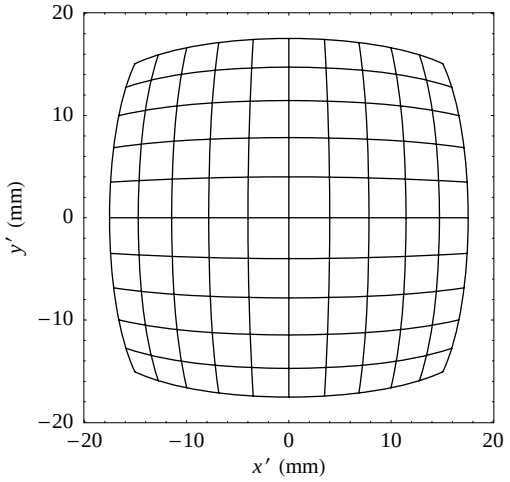

Figure 3.37 Barrel distortion.

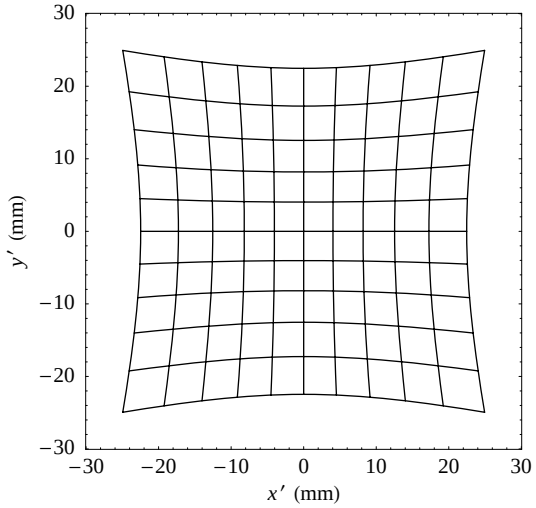

Figure 3.38 Pincushion distortion.

3.5 Optical Path

The optical path is defined as the index of refraction of the medium times the path length traveled by the ray in the medium. Therefore, in Figure 3.39, the optical path of the tray traveling from object point P to P_1 to the image point P' (on the paraxial image plane) is

$$nT + n'T' \tag{3.116}$$

We want to calculate this path length to third order.

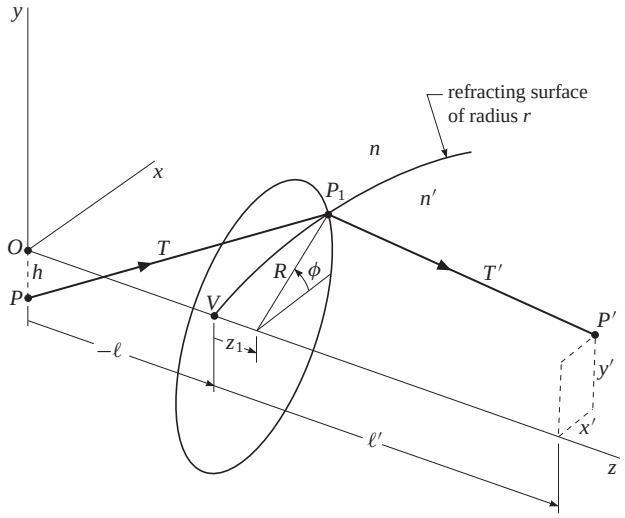

Figure 3.39

We start with Equations 3.7, which we restate for convenience:

$$T = -\ell\sqrt{1 + x} \tag{3.117a}$$

where

$$x = \left(\frac{1}{\ell} - \frac{1}{r}\right)\frac{R^2}{\ell} - 2\sin\phi\,\frac{Rh}{\ell^2} + \frac{h^2}{\ell^2} + \text{O}(s^4) \tag{3.117b}$$

We use the binomial power series Equation 3.1 to expand Equation 3.117a to get

$$T = -\ell\sqrt{1+x} = -\ell\,(1+x)^{\frac{1}{2}}$$
$$= -\ell\left[1 + \frac{1}{2}x + \mathrm{O}(x^2)\right] \tag{3.118}$$

Multiplying T in Equation 3.118 by the index of refraction n, and using Equation 3.117b to substitute for x, we have the power series for the optical path from P to P_1

$$nT = -n\ell - \frac{n}{2}\left(\frac{1}{\ell} - \frac{1}{r}\right)R^2$$
$$+ \frac{n}{\ell}\sin\phi\, Rh - \frac{n}{2\ell}h^2 + n\ell\,\mathrm{O}(s^4) \tag{3.119}$$

To obtain $n'T'$, the optical path from P_1 to P', we develop a power series expression for T' by going back to Equation 3.35

$$T' = \frac{\ell' - z_1}{\gamma'} \tag{3.120}$$

Substituting Equation 3.4 for z_1, and Equation 3.39 for $1/\gamma'$, we get

$$T' = \left[\ell' - \frac{R^2}{2r} - r\mathrm{O}(s^4)\right]$$
$$\left[1 + c_1R^2 + c_2Rh + c_3h^2 + \mathrm{O}(s^4)\right]$$
$$= \ell' + \left(\ell' c_1 - \frac{1}{2r}\right)R^2$$
$$+ \ell' c_2 Rh + \ell' c_3 h^2 + \ell'\,\mathrm{O}(s^4) \tag{3.121}$$

Because P' is on the paraxial image plane, we can use Equations 3.53 to substitute for c_1, c_2, c_3 in Equation 3.121 to obtain $n'T'$:

$$n'T' = n'\ell' + \frac{n'}{2}\left(\frac{1}{\ell'} - \frac{1}{r}\right)R^2$$
$$- \frac{n}{\ell}\sin\phi\, Rh + \frac{n^2\ell'}{2n'\ell^2}h^2 + n'\ell'\,\mathrm{O}(s^4) \tag{3.122}$$

where we have also used $\mu = n/n'$.

When we add together Equations 3.119 and 3.122, we see that the $\sin\phi\, Rh$ terms cancel, and so

$$nT + n'T' = -n\ell + n'\ell' + \frac{1}{2}\left(-\frac{n}{\ell} + \frac{n'}{\ell'} - \frac{n'-n}{r}\right)R^2$$
$$- \frac{1}{2}\left(\frac{n\ell'}{n'\ell}h\right)\left(-\frac{n}{\ell} + \frac{n'}{\ell'}\right)h$$
$$+ (n\ell + n'\ell')\,\mathrm{O}(s^4) \tag{3.123}$$

We observe that the coefficient of R^2 is zero by the object-image relation of Equation 3.45e. Using Equation 3.47 to introduce h', Equation 3.123 becomes

$$nT + n'T' = -n\ell + n'\ell' - \frac{1}{2}\left(-\frac{n}{\ell} + \frac{n'}{\ell'}\right)hh'$$
$$+ (n\ell + n'\ell')\,\mathrm{O}(s^4) \tag{3.124a}$$

An alternative form of this equation is obtained when Equation 3.45e is used on the coefficient of hh' to give

$$nT + n'T' = -n\ell + n'\ell' - \frac{1}{2}\left(\frac{n'-n}{r}\right)hh'$$
$$+ (n\ell + n'\ell')\,\mathrm{O}(s^4) \tag{3.124b}$$

Looking at Equations 3.124, we see that there are no third order terms. Therefore, we can say that the optical path, $nT + n'T'$, between an object point and the corresponding image point is independent of R through the third order. In other words, no matter what path a ray travels between the object and image points, the optical path is a constant through the third order; the R dependence does not show up until the fourth order terms are included. The fact that the optical path between object and image is a constant to a high degree of approximation is a very useful one.

Problems

3.1 (a) Obtain the power series for z_1 in Equation 3.4 to the R^4 term; that is, get the next term beyond the R^2 term. (b) In your new power series, the O term involves what power of s?

3.2 In Equation 3.4, suppose $r = 100\,\text{mm}$ and $R = 10\,\text{mm}$. Calculate (a) the exact value of z_1, (b) the approximate value given by the first term of Equation 3.4, and (c) the better value given by your power series in the previous problem.

Note: In this chapter, some of the algebraic steps in the derivation of certain equations were not always shown. In the problems that follow, show all the steps.

3.3 (a) Equation 3.8 for α, (b) Equation 3.9 for β, and (c) Equation 3.10 for γ.

3.4 Equation 3.15.

3.5 Equation 3.19.

3.6 Equation 3.25.

3.7 Equations 3.27.

3.8 Equations 3.29.

3.9 Equations 3.31.

3.10 Equation 3.55.

3.11 Equation 3.58.

3.12 Equation 3.61.

3.13 Equation 3.63.

3.14 Equation 3.69.

3.15 Equation 3.71.

3.16 Equation 3.105.

3.17 Equation 3.119.

3.18 Equation 3.122.

3.19 Equations 3.124.

Note: In the problems that follow, use $n = 1$, $n' = 1.5$, $\ell = -300\,\text{mm}$, $\ell' = 900\,\text{mm}$, $h = -9\,\text{mm}$, $h' = 18\,\text{mm}$, $r = 100\,\text{mm}$, $R = 10\,\text{mm}$, and $\phi = 120\,\text{deg}$.

3.20 Show that the given values satisfy (a) the object-image condition of Equation 3.45e, and (b) Equation 3.47.

3.21 Calculate D_{SA} from Equation 3.56.

3.22 Calculate D_{CM} from Equation 3.62.

3.23 Calculate D_{AT} from Equation 3.72.

3.24 Calculate D_{CR} from Equation 3.70.

3.25 Calculate D_{DS} from Equation 3.106.

3.26 Calculate x'_{SA} and y'_{SA} from Equations 3.55 and 3.58.

3.27 Calculate x'_{CM} and y'_{CM} from Equations 3.61 and 3.63.

3.28 Calculate x'_{AC} and y'_{AC} from Equations 3.69 and 3.71.

3.29 Calculate x'_{DS} and y'_{DS} from Equations 3.103 and 3.105.

3.30 Based on Equations 3.49 and 3.50 of third-order aberration theory, the image point P' on the paraxial image plane has the coordinates

$$x' = x'_{AS} + x'_{CM} + x'_{AC}$$

and

$$y' = h' + y'_{AS} + y'_{CM} + y'_{AC} + y'_{DS}$$

Using the given values and the values calculated in the previous problems, determine (a) x', (b) y', and (c) for better comparison with the corresponding value in the next problem, $y' - h'$.

3.31 (a) Determine the exact value of z_1. (b) Determine the endpoints of T referenced to the origin O (see Figure 3.2). (c) Calculate the exact value of T using Pythagorean's theorem. (d) Calculate the exact values of α, β, and γ. (e) Using the flow chart in Figure 2.19, trace the ray exactly from P to P_1 to P'; that is, determine T; x_1, y_1, z_1; α', β', γ'; T'; x', y', z'; and $y' - h'$. (f) Compare the approximate values of x', $y' - h'$ calculated in the previous problem with the exact values; that is, determine the percentage error to two significant figures by using the formula

$$\text{error} = \frac{|\text{approximate value} - \text{exact value}|}{\text{exact value}} \times 100\%$$

Remember that by "exact" we mean an equation is used where there are no approximations in its derivation.

3.32 (a) Use Equation 3.124a or Equation 3.124b to calculate the optical path $nT + n'T'$. (b) Use the exact values determined in the previous problem, and calculate the exact value of $nT + n'T'$. (c) Calculate the percentage error.

Page intentionally left blank.

Chapter 3: Answers to Problems

Note: All the calculations are made with *Mathematica*'s 16 decimal digit precision and the results are usually displayed to six decimal digits, unless the digits to the right of the decimal point are trailing zeros, then they are not printed.

3.1 (a) $\frac{R^2}{2r} + \frac{R^4}{8r^3}$; (b) 6

3.2 (a) 0.501256, (b) 0.5, (c) 0.50125

3.20 (a) $0.005\,\text{mm}^{-1}$, $0.005\,\text{mm}^{-1}$; (b) 18 mm, 18 mm

3.21 $0.000217284\,\text{mm}^{-2}$

3.22 $0.0000271605\,\text{mm}^{-2}$

3.23 $6.79012 \times 10^{-6}\,\text{mm}^{-2}$

3.24 $6.17284 \times 10^{-6}\,\text{mm}^{-2}$

3.25 $7.71605 \times 10^{-7}\,\text{mm}^{-2}$

3.26 0.108642 mm, −0.188173 mm

3.27 0.042339 mm, −0.122222 mm

3.28 0.01 mm, −0.0363731 mm

3.29 0 mm, −0.0045 mm

3.30 (a) 0.160981 mm, (b) 17.6487 mm, (c) −0.351269 mm

3.31 (a) 0.501256 mm,
(b) (0, −9, 0) mm, (−5, 8.66025, 300.501) mm
(c) 301.061 mm
(d) −0.0166079, 0.05866, 0.99814
(e) 301.061 mm;
−5 mm, 8.66025 mm, 0.501256 mm;
0.00573767, 0.00999156, 0.999934 rad;
899.558 mm
0.161368 mm, 17.6483 mm, 0 mm;
−0.351749 mm;
0.24 %, 0.14 %

3.32 (a) 1650.405 mm, 1650.399 mm; (b) 0.0004 %